INSTITUTE OF
PAPER CHEMISTRY
Appleton · Wisconsin

THE TENSILE FRACTURE BEHAVIOR OF LARGE
PAPER SPECIMENS CONTAINING EDGE CUTS

Project 3219

Report One
A Progress Report
to
MEMBERS OF THE INSTITUTE OF PAPER CHEMISTRY

October 25, 1977

THE INSTITUTE OF PAPER CHEMISTRY

Appleton, Wisconsin

THE TENSILE FRACTURE BEHAVIOR OF LARGE PAPER
SPECIMENS CONTAINING EDGE CUTS

Project 3219

Report One

A Progress Report

to

MEMBERS OF THE INSTITUTE OF PAPER CHEMISTRY

October 25, 1977

TABLE OF CONTENTS

THE INSTITUTE OF PAPER CHEMISTRY

Appleton, Wisconsin

THE TENSILE FRACTURE BEHAVIOR OF LARGE PAPER
SPECIMENS CONTAINING EDGE CUTS

SUMMARY

A study was undertaken of the tensile fracture behavior of paper webs containing single edge cuts of different length. The major portion of the study was conducted on specimens 0.381 meter in width and 2 meters in length. Samples of web-offset, bond, specialty kraft, and bag paper were evaluated at 50% RH. Edge cut lengths were varied within the range of 3 to 100 mm. The bond paper was also tested at relative humidities of 12, 77, and 85% RH and at 50% RH after preconditioning at 85% RH.

The relationship between the critical stress at rupture, $\sigma_c t$, and the initial cut length, $\underline{a}$, proved to be complex. Two different regimes of behavior could be identified in tests at 50% RH. The large-cut-length regime included initial cut lengths from about 20 to 100 mm. Within that regime, the stress-strain response of specimens containing edge cuts was Hookian to the point of fracture of the specimen. Critical stresses within the large-cut-length regime could be related to the initial cut length by a power law as follows:

$$\sigma_c t = \beta \, a^{\alpha}$$

The value of the exponent, α, was approximately -0.37 for the kraft and bond papers at 50% RH and about -0.3 for the web-offset paper. The product of the critical stress and the square root of the initial cut length increased appreciably as the initial cut length increased, indicating apparent nonconformance with the linear elastic fracture theory. Constancy in the product could not be attained by the application of simple plasticity corrections or finite-specimen-size correction factors.

A small-cut-length regime was identified as embracing initial cut lengths of up to about 8 mm. Within this regime the same power law relationship fit the data quite well with exponents approximately the same as those for the large-cut-length regime; however, the curve for small cut lengths was shifted upward on the critical stress axis by a multiple of 1.2 to 1.25 at 50% RH. The small-cut-length regime is further characterized by the appearance of nonlinearity in the stress-strain response of specimens containing edge cuts. A transitional region connects the two regimes over the cut length range of about 8 to 20 mm.

The identification of regimes of response based on initial cut lengths is convenient for the presentation and empirical analysis of data. Such regimes were distinct in the tests at 12% RH, but not apparent in tests at 77 and 85% RH, where a single power law relationship applied quite well over the entire experimental range of cut lengths.

The critical stress at a small cut length in tests at 12% RH was about the same as that obtained at 50% RH, and greater than those obtained at 77 and 85% RH. At large cut lengths, however, the critical stress at 12% RH fell below values obtained at either 50 or 77% RH. This behavior was associated with the higher extensional stiffness and lower in-plane tearing strength of the bond paper at 12% RH relative to the other test conditions.

The critical stress of all samples at all testing conditions at an initial cut length of 3.3 mm was shown to be proportional to the product of the machine-direction extensional stiffness and the cross-direction in-plane tearing strength raised to the 0.233 power. At a cut length of 48 mm, the critical stress was more nearly proportional to the square root of the product of the machine-direction extensional stiffness and the cross-direction in-plane tearing strength.

Such empirical correlations indicate that the critical stress in the small-cut-length regime relates rather strongly to the machine-direction extensional stiffness, only weakly to the in-plane tearing strength, and presumably only weakly to other parameters involving energy in fracture. At large cut lengths, energy parameters become more important, conforming better to the expectations of linear elastic fracture mechanics theory. Overall, linear elastic fracture theory does not describe the results of these fracture tests on paper and a simple means for improving the applicability of this theory is not at hand.

The relationships between critical strain and initial cut length were somewhat simpler to describe but not easier to interpret. All samples showed rather similar critical strain versus initial cut length behavior. The approximate and principal effect of changing moisture content was to change the critical strains at all cut lengths by the same factor.

Assuming equivalent naturally-occurring flaw dimensions, a method for comparing the runnability quality of paper samples is proposed based on the computation of "strain allowance." Strain allowance is the difference between the critical strain at which a rupture will occur and the operating strain at a desired web tension level. In the particular example chosen, the disadvantage of low moisture content levels on strain allowance is clear. Greater strain allowances represent greater factors of safety and are attained at higher moisture contents at the expense of lower extensional stiffness and yield stress levels. A sample preconditioned at 85% RH and tested at 50% RH had a strain allowance equal to that of a sample tested at 77% RH and is preferred, therefore, because of its higher extensional stiffness and yield stress. Best web runnability is likely to be attained by reducing tensions during drying to attain high strain allowance values at intermediate moisture content levels.

The effect of length to width ratio on tensile fracture behavior was studied on specimens of bag paper of 381-mm width. The critical stress was particularly sensitive to changing length/width ratio at ratios of 1 or less and may approach limiting low values at large ratios. Such length/width ratio effects were noted at various initial cut lengths. The intensification of stress at edge cuts became negligible as the specimen length/width ratio was reduced to 0.26. However, at this low ratio, the critical stress became unusually sensitive to cuts within the central region of the web. Such results indicate that length/width ratio effects, and perhaps length and width dimensions generally, could be quite important in the evaluation of web runnability on different converting apparatus.

Measurements of the velocity of running cracks in web-offset paper were made by an electrical resistance method. At an edge-cut length of 3.18 mm, the crack velocity accelerated rapidly and reached a maximum of about 1000 meters per second. As the velocity exceeded 700 meters per second, crack branching became prevalent indicating the brittle nature of paper. At an initial cut length of 12.7 mm, rapid acceleration occurred 80 to 100 mm from the tip of the initial cut. At 50.8 mm, no rapid acceleration was noted over the remaining width of the specimen, and the maximum velocity recorded in three such tests was about 4 m/sec. The general behavior of running cracks in paper is not unique, but rather conforms to the crack propagation behavior of many metals and plastics.

INTRODUCTION

A principal objective of this project is to develop a better understanding of the in-plane tensile strength of paper relative to to its end uses. Of major interest are "web breaks" in paper manufacturing or paper converting apparatus. Papers exhibiting a high frequency of web breaks are referred to as having poor "runnability". It has long been appreciated that webs will break occasionally at tensile stress and strain levels well below the nominal values obtained by testing small specimens in the laboratory. Though infrequent, such breaks nonetheless present a serious problem.

Sears, et al (1) have shown that newsprint webs of 15-inch width failed in dynamic web-transport situations at a ten-times-greater frequency as the strain increased by 0.06% in the range of 0.3 to 0.4% total strain. The breaks could be traced in most instances to the presence of shives in the newsprint sheet, and particularly to shives located near or at the edge of the web. The shive represents a "flaw" in the structure at which stress can be intensified. The magnitude of the intensified stress may be sufficient to initiate fracture of the web, though the average stress remote from the flaw may be relatively low.

There are two approaches to the problem of improving runnability other than adjusting the converting process to impose a less severe stress or strain condition. The most obvious, of course, is to reduce the number and size of flaws in the sheet. The second is to improve the ability of the sheet to withstand a greater load or strain when a flaw of a particular size is present. The prevailing view in this respect seems to be that better runnability will be attained if the stretch of the sheet is improved either through increasing the moisture

content of the sheet or by permitting greater shrinkage during drying. Both approaches are of commercial interest since both are feasible. It has not been easy to confirm this view by monitoring web runnability performance in use, since constancy in flaw size and distribution in different samples cannot be assured.

If one is to fully understand the practical strength of materials, the matter of how the stress-strain fields within a specimen under load are altered by the presence of a flaw should be known. This is extremely difficult to establish experimentally. It is relatively easy on the other hand to introduce flaws of any desired size, shape, and orientation into specimens and to observe their effect on strength. This is the approach which was taken in this study. The orientation and position of the flaw was held constant; only the flaw dimension was changed. By working with different samples and at different moisture contents, the range of information obtained was extended considerably.

The literature dealing with the fracture behavior of materials is quite extensive. There are, however, very few studies recorded in the literature which deal with the fracture properties of paper. The two earliest attempts to examine paper from the point of view of fracture mechanics theory are those of Balodis (2) and Andersson and Falk (3). In both of these studies, specimens only a few centimeters wide were tested and no attempts were made to determine whether the small-specimen results were consistent with the tensile behavior of large specimens.

Recently, Seth and Page (4, 5) carried out a more extensive study of paper fracture on large specimens employing the techniques and principles of fracture mechanics. They showed that at a relatively large flaw size the stress

at which fracture occurred decreased as the specimen width increased (same length
to width ratio), apparently approaching a minimum limiting value asymptotically.
The specimen size effect became small at a specimen width of 15 inches — the
width employed in our study. Prior to undertaking our work, we established
that the results obtained on small specimens did not agree with the results
of large-specimen tests and that no simple empirical correlation of small-specimen
and large-specimen results was apparent. The decision to proceed with the testing
of webs 15 inches in width was made largely on the basis of expediency, but
with the knowledge that the results would not be much different if wider webs
were tested.

It should be noted that the paper industry has long looked to tensile
strength and tearing energy as indicators of paper quality which are expected
to relate to performance in use. There is yet too little understanding of how
these two properties are to predict performance in use. The "runnability" of
paper webs is an excellent case in point.

FRACTURE MECHANICS

Fracture mechanics deals with the strength of materials in relationship to specimen size and shape, the dimensions, location, and orientation of flaws in the specimen, and the inherent mechanical properties of the material. This brief introduction to fracture theory should be helpful to the reader of this report who is not familiar with the subject. The more serious reader may consult any of a number of textbooks [for example, (6, 7)] and various reviews of the published literature [such as (8)]. The following comments are drawn from such published literature.

Any uniform material subjected to an external load will at any instant of time have a particular distribution of stress and strain, the form of which is dependent on the shape of the specimen, the nature of the external forces and constraints, and the characteristic mechanical properties of the material. Most materials do not have uniform structures. Structural nonuniformities, ranging from the molecular to the grossest macroscopic dimension, contribute to the nonuniformity of stress and strain throughout the material. Although one would like to measure the variations in stress and strain throughout the material, this is ordinarily difficult at best and at some levels impossible. Because of structural heterogeneity, stresses will be high in some regions within a specimen and lower in others. Fracture will begin whenever any local stress exceeds the material strength at that point, even though the material is not stressed generally to a critical level.

It is sometimes possible to identify and characterize naturally-occurring "flaws" in a material and to observe these under load with the view that fracture will be initiated at those sites. Naturally-occurring flaws are

obviously quite important in materials since their elimination or a reduction in
their frequency of occurrence or size may lead to improved load-carrying capacity.
On the other hand, it is most difficult to study the fracture of materials
employing only their natural flaws. Flaws of particular interest in fracture
mechanics are discontinuities in structure over which stresses cannot be trans-
ferred. Flaws of this kind are better introduced deliberately in a material,
since one can then completely control the flaw dimensions, flaw orientations,
etc. Flaws can, of course, have any desired initial form. They are usually
chosen to conform to one's capability for theoretical analysis, and generally
will have a simple shape which is easily introduced. A most common flaw is a
cut or crack in the material. In paper, the simplest cut extends throughout
the entire thickness of the sheet.

For a specimen containing a cut (crack) of particular size, it is
customary to refer to the average stress (at points distant from the cut) needed
to initiate fracture as a "critical stress." Conversely, at any particular
stress level, the smallest cut dimension at which fracture is induced to begin
is the "critical crack" size. Lower critical stresses are expected at larger
crack lengths. If a crack deliberately introduced does not produce fracture
(e.g., the fracture occurs elsewhere), this is taken to indicate that the
naturally-occurring flaws are dominant and probably of larger dimension. By
seeking the dimension of the smallest introduced crack at which fracture regularly
occurs, one can estimate a "characteristic dimension" of naturally-occurring
flaws. Because of its fiber network structure, paper really is a continuous
array of flaws of macroscopic size. Thus, the smallest cut needed to initiate
fracture at the cut in such structures may be rather large compared with more
homogenous materials.

The naturally-occurring flaws in a material (such as paper) have various sizes, shapes, orientations, etc. Though flaws of large size may occur rather infrequently, they are expected to determine the frequency with which samples of the material will break at low levels of stress. In the transport of paper webs, new material is continually being brought to a particular operating stress level and, in effect, under ideal conditions one is then practicing a program of continuous web testing. The observed frequency of web breaks is an indicator of the frequency of occurrence of flaws of critical size or larger for that stress and strain level. As noted earlier, in order to reduce the web break frequency, one must either reduce the size or number of the naturally occurring flaws or, through changes in material properties, develop greater resistance to fracture at any given flaw condition. Such paper quality improvement might be used to reduce the web break frequency or, alternatively, to achieve savings via redesign of the product (as by reducing the basis weight) without increasing the break frequency.

A defect or flaw in a material, particularly one over which stress cannot be transferred either totally or partially, acts as a stress intensifier. At particular points about the periphery of the flaw, the stress rises to values above that in the specimen more remote or distant from the flaw. The magnitude of this stress intensification effect and the factors which affect it are of particular interest. The simplest approach in the evaluation of stress intensification is to measure the loss in ultimate strength of specimens when flaws of different kinds are introduced. It is assumed that a specimen will always break when the local intensified stress reaches a particular constant value, independent of flaw size. The ratio of the stress at rupture of specimens without flaws to the stress at rupture when a flaw is present is the stress intensification

factor commonly employed in engineering. While simple in concept, this approach quickly becomes more complicated when proper accounting is desired for the shape, dimensions, and orientation of flaws. Obviously, testing can be performed in a number of different modes: tensile, bending, shear, etc.; and different stress intensification factors will ordinarily be obtained in the different modes. In the following discussion, only the tensile mode is considered.

LINEAR ELASTICITY THEORY

The magnitude of stress intensification is affected by the manner in which a material responds to external loads. This involves stress, strain, and time as variables and one ordinarily thinks of the implications of plastic flow, yield stresses, creep, stress relaxation, etc. The development of theory in fracture mechanics must consider, of course, the influence of all such effects on stress intensification if they are present. Unfortunately, when materials exhibit "plastic" or "viscoelastic" behavior (time-dependent behavior), prediction of the stress-strain distribution in a body containing a flaw becomes exceedingly difficult. It is not surprising, therefore, that the early development and use of theory involved materials which exhibit only <u>immediate linear elasticity</u> when subjected to load. Immediate elasticity connotes behavior in which the stress is linearly proportional to the strain (Hookian response) and for which total recoverability of strain occurs upon removal of the stress. Linear elastic theory can be employed to calculate the distribution of stress and strain in specimens containing discontinuities, such as holes or sharp-edged cracks. Calculations were made first for specimens of infinite size containing either a single crack or a regular array of cracks. Further analysis is possible to include the effects of finiteness of specimen size. It should be made clear at the outset that most structural engineering materials (and paper) do not

conform to the assumption of linear elasticity as the sole mode of response
to an external load. The departure from linear elasticity, however, may not
be large in many instances; and linear elastic fracture theory may be applicable
to such materials. It is common practice, therefore, to compare the observed
fracture response of a material with the predictions of the linear elastic
fracture theory simply to establish the applicability of or the degree of de-
parture from the theory.

The Stress Intensity Approach

Perhaps the most relevant of the various linear elasticity analyses
deals with the stress field surrounding the tip of a sharp-edged crack oriented
perpendicular (in the x-direction) to the direction of the tensile stress (the
y-direction) in thin planar or sheetlike specimens of infinite size. Various
points in the plane are identified by their distance from the crack tip, r, and
angle, θ, to the x-axis (the direction in which the crack is expected to propa-
gate or grow). Linear elasticity theory predicts the stresses at those points
(σ_x and σ_y, in the x and y-directions). For small distances from the crack tip,
the result is as shown in Equation (1).

$$\sigma_x \text{ or } \sigma_y = \frac{K_1}{(2\pi r)^{1/2}} F(\theta) \qquad (1)$$

In the above expression, the function, $F(\theta)$, is different for the x-
and y-direction stresses. K_1 is the stress-intensity factor, a property of
the material, which is defined as follows.

$$K_1 = C_1 \sigma (a)^{1/2} \qquad (2)$$

The stress, σ, is that existing in the body of the specimen so remote from the crack that it is not influenced by the presence of the crack. The term $\underline{a}$ is the crack length dimension and $\underline{C_1}$ is a constant which depends on the specimen size, on whether the cracks are placed in the body of the specimen or at a free surface, etc. For an infinite specimen with a centrally positioned crack, $\underline{C_1}$ is equal to $(\pi)^{1/2}$. Correction factors, $\underline{F}(\underline{a}/\underline{b})$, have been calculated and tabulated for edge and center cracks of various lengths, $\underline{a}$, relative to a characteristic specimen width dimension, $\underline{b}$. The constant $\underline{C_1}$ may then be replaced by $(\pi)^{1/2}\underline{F}(\underline{a}/\underline{b})$.

These equations predict that the stress at any constant angular orientation to the crack tip is inversely proportional to the square root of the distance from the crack tip and approaches infinity at the tip of a sharp crack. The stress cannot, of course, reach levels exceeding the cohesive strength of the material. One must also consider, for example, that materials will exhibit various degrees of blunting or rounding of the crack tip. Even though the intensified stress can reach only a particular maximum value at the crack tip boundary in any given material, the form of the stress distribution about the crack tip may follow Equation (1).

The most significant implication of the theory, obtained by substituting for $\underline{K_1}$ in Equation (1), is that for any critical level of tensile stress at which fracture occurs the product of that stress, $\sigma_{\underline{c}}$, and of $(\underline{a})^{1/2}$ is constant. Both of these are experimental quantities and one can easily test for the condition of constancy. The crack length of interest is that which exists at the instant of unstable fracture rather than the length of the crack originally introduced. When constancy in the product $\sigma_{\underline{c}}(\underline{a})^{1/2}$ is noted, it can be taken as evidence that the linear elastic facture theory is applicable if the material also exhibits apparent elastic behavior under load to the point of fracture.

Elastic materials can fracture only in the "unstable mode," in which fracture begins suddenly and progresses rapidly to completion in a specimen under fixed external restraint. Unstable fractures are commonly referred to as "brittle" fractures. Materials which fracture in the unstable mode (if only under some conditions of testing) are often referred to as brittlelike. Some materials may fracture in a "stable" mode. Stable fractures do not proceed to completion under constant external restraint (fixed clamps). Rather, one must steadily increase the average overall specimen strain if crack growth is to continue. Paper will respond in both modes, depending on the test conditions and perhaps on the material properties.

Energy Criteria for Fracture

If a flaw exists in a material subjected to external load as, for example, a cut or crack in a paper web, two criteria must be met before the crack will grow or propagate. First, the level of the intensified stress (usually a maximum at the tip of the crack) must exceed the strength of the material at that point. This condition must continue to be met, of course, if fracture is to continue. The second criterion in a spontaneous fracture process is that the energy required for fracture (dissipated as the crack grows) must be made available from the stored elastic strain energy within the stressed specimen. This criterion must also continue to be met as the crack propagates. In theory, the two criteria are directly and easily related for totally elastic materials.

A complete description of the strain-strain distribution within an elastic body containing a crack also completely defines the stored elastic strain energy of the body. The strain energy can, in principle, be calculated

for any critical stress and crack length condition. It is further possible,
for a given condition of external specimen restraint (for example, fixed clamp
positions), to calculate the change in the strain energy for an infinitesimal
change in crack length. This is defined as the <u>strain energy release rate</u> and
designated as <u>G</u>. It is, for elastic materials, directly proportional to the
stress intensity factor, K_1. For the case of <u>plane stress</u>, and for isotropic
materials, the relationship has the simple form shown in Equation (3), with the
subscript <u>c</u> indicating the values at the critical level of incipient unstable
fracture.

$$G_c E = K_c{}^2 \tag{3}$$

More complex expressions apply to anisotropic or orthotropic materials,
retaining the general relationship between the energy release rate and the square
of the stress-intensity factor, but with substitution of a more complex function
of the elastic constants for the Young's modulus, <u>E</u>.

The critical stress-intensity factor, <u>K</u><u>c</u>, can be replaced with its
equivalent [from Equation (2)], yielding

$$G_c E = C_1{}^2 \sigma_c{}^2 a \tag{4}$$

This is the familiar form of the relationship between crack length,
critical stress, and Young's modulus, which is often presented in discussing the
energy criteria for fracture. The energy release rate is also referred to as
"fracture energy" or as "crack extension force."

The energy criteria of fracture are embodied simply in the statement
that unstable fracture will occur if the decrease in the elastic strain energy

of the system (the specimen in fixed grips) for an infinitesimal increase in crack length just exceeds the energy required for extension of the crack.

There is often little if any advantage in choosing the energy criteria over the stress-intensity approach. It does not, for example, overcome any difficulties which may arise because of inelastic behavior. On the other hand, there is considerable interest in measuring the resistance of paper to fracture by tearing-type tests. No tearing test, however, can duplicate the conditions of resistance to fracture that exist in the in-plane tensile straining of paper. The appeal of energy criteria in fracture is considerable if fracture energy or fracture resistance values can be obtained experimentally much more easily than can the stress-intensity factors. It must be demonstrated, however, that reasonable predictions of stress-intensity factors can be made from energy parameters for all conditions of practical interest. Seth and Page (4, 5) have shown that a stress-intensity factor determined under specific geometric conditions, with empirical crack length corrections to account for plasticity and considering paper as an elastic orthotropic body, yields critical strain energy release rates equivalent in magnitude to a fracture resistance energy value determined experimentally in the "stable" fracture of paper specimens.

Plasticity Effects

Materials which show appreciable inelastic strain in response to external loads present special problems in fracture mechanics. If the degree of inelastic straining is small, their fracture behavior may be in substantial accord with linear elastic fracture theory. If plasticity is appreciable, however, such theory may not describe the material behavior at all. Various techniques for dealing with plasticity have been developed and this is a subject of considerable current interest.

Where plastic or viscoelastic behavior is significant, but small,
regions beyond a certain distance from the crack tip may remain elastically
stressed, whereas near the crack tip a region exists where a transition occurs
between the elastic and plastic response. In the plastic region, the strains
are greater than predicted by the existing stresses and are time-dependent as
well. The stress at the boundary is, of course, the yield stress. As the crack
propagates, strain energy from the elastic field is transferred to the plastic
region where energy dissipation occurs. If the elastically stressed region
has the stress distribution of the linear elastic theory and if negligible strain
energy release occurs from within the plastic region, then the equivalence of
an energy release rate (from an elastic stress field) to the fracture energy
requirement will still be a proper fracture criterion. The essential principles
of linear elastic fracture theory may apply, but the effective crack length will
then be greater than the actual length of the crack. Plasticity corrections often
involve replacement of the actual crack lengths with "corrected" or effective
crack lengths.

If the average stress level within the net (uncut) section of the
specimen approaches or exceeds the yield stress, constancy in the stress intensity
factor, K_c, is not to be expected. The usual approach in testing is to select
specimen dimensions and crack lengths sufficiently large so the net section
stress falls safely below the yield stress. In the testing of metals, a net
section stress less than about 80% of the yield stress is considered safe.

The general effect of plasticity in fracture is to reduce the ratio of
the intensified stress at the crack tip to the average stress of the specimen.
The load-carrying capacity of a specimen will be greater as a result. A combination
of high cohesive strength along with high plasticity should provide for best
resistance to fracture.

EXPERIMENTAL

The following experimental approach was employed in this study. Sharp cuts of different lengths were introduced at one edge of large specimens of commercial paper. The tensile behavior of specimens containing such edge cuts was then determined and related to the initial cut dimensions. A single cut was introduced at one edge only, perpendicular to the direction of loading and mid-distant between the clamps. The appropriate geometry and nomenclature are shown in Fig. 1.

It was established prior to this study that tensile fracture data obtained using small specimens differed from the results of large-specimen tests. In the interest of developing data having maximum relevance to the tensile behavior of paper webs on commercial converting apparatus, the first studies were conducted using webs 381 mm wide (15 inches) with an initial test span of 1270 mm (50 inches). These were the largest specimens which could be accommodated in the available Baldwin tensile testing apparatus at a specimen length to width ratio of 3:1 or greater. Following the construction of the Large-Specimen Tensile Testing apparatus (LSTT), the test span was increased to 2000 mm (78.7 inches); the width remained the same.

The rate of straining was held constant throughout the study at 6% per minute in the Baldwin tests and 5% per minute in the LSTT tests. The difference in these two rates of straining is expected to be negligible. Rate of straining, however, is a variable of considerable interest in paper fracture behavior. For example, the rate of straining in dynamic web transport can be extremely high — much higher than can be developed in conventional load-elongation tensile testing apparatus. The nominal 5% per minute constant rate of straining
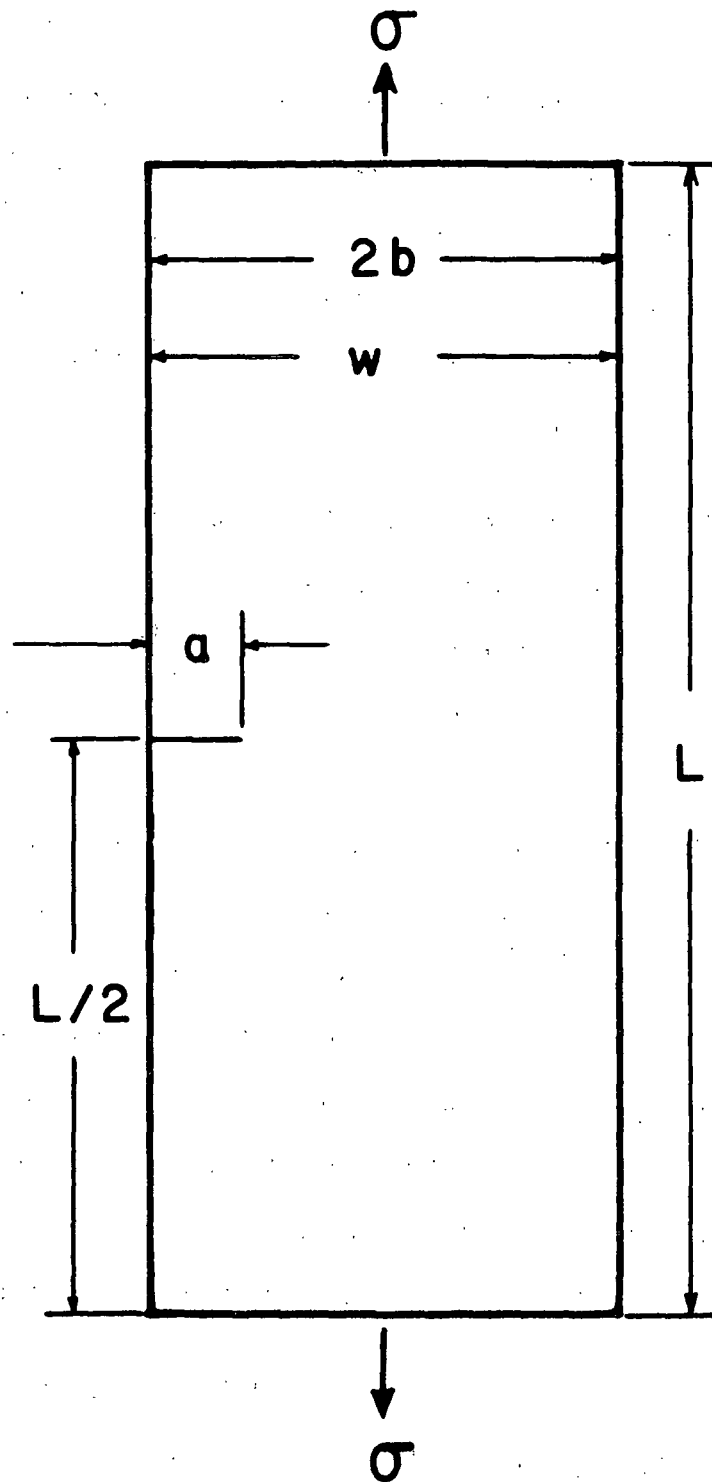
Figure 1. A Single-edge Crack of Length a in a Specimen of
Finite Size Subjected to Tension

was selected to ensure accurate plotting of the load-elongation response of the specimens.

The initial cuts were introduced into the specimen edge after the specimens had been properly aligned and clamped for testing. This is important since precutting of specimens precludes accurate clamping and alignment. All cuts were made using a sharp razor blade. The end of the cuts terminated randomly in the specimens; i.e., sometimes falling in dense areas of heavy basis weight and sometimes in lightweight regions.

The introduction of sharp-edge cuts, though convenient experimentally, might be viewed as producing flaws which are never present in commercial paper and, thus, not representative of naturally-occurring flaws. It should be noted, however, that the extremely sharp edge of the razor cut is not retained to the point of incipient specimen rupture. Rather, as the load increases, the cut opens slightly and the fiber network at the cut tip suffers some debonding and structural disintegration. The result just prior to complete failure of the specimen is a somewhat damaged and blunted crack tip which undoubtedly differs in detail for different papers. Local debonding at the tip of a sharp cut or other flaw is characteristic of the paper fracture process. It is preferable in initial studies that the tip of an introduced flaw be sharper initially than that which results after straining of the specimen to near rupture. This condition is met adequately by making the initial cuts with a sharp blade.

The reduction in the load-carrying capacity of paper webs of large length-to-width ratio is greatest when a flaw of particular length is present at the edge of the specimen and oriented perpendicular to the direction of loading (as employed in this study). The experimental work was confined to flaws of this kind.

Four different commercial papers, from four different manufacturers, were evaluated in this study. The samples are identified as follows:

web-offset paper

kraft paper - supercalendered, unbleached

bond paper

bag paper - unbleached southern pine kraft

All of the samples were supplied as rolls of 15-inch width. The kraft paper was evaluated immediately upon receipt. The remaining samples were stored in roll form for many months prior to sampling.

In all cases, specimens were cut from the parent rolls in a 50% RH atmosphere. It is believed that in all cases the specimens gained moisture upon exposure to this atmosphere. The specimens were stored in flat stacks for a period of many weeks prior to testing. This permitted any relaxation, creep recovery, or other dimensional and structural changes to occur prior to testing. The kraft paper had a doubtful moisture history and was preconditioned at 85% RH for 48 hours before reconditioning and testing at 50% RH.

The specimens of each set were numbered randomly on removal from the sample roll, then selected for testing in numerical order. The object of this was to minimize problems due to possible machine-direction variations in paper properties. A summary of the principal tests performed on the four different samples is given in Table I.

In addition to the large-specimen testing, the samples were tested in the laboratory using standard test methods. The results of these evaluations are summarized in the appendix of this report. Attention is directed to the evaluation of the machine-direction (MD) tensile properties across the

15-inch width of the webs. Ash content and fiber length distributions were

also determined for all samples.

TABLE I

SUMMARY OF LARGE-SPECIMEN TENSILE TESTS

Sample Set	Paper Grade	Basis Weight, g/m^2	Specimen Size, mm	Apparatus	Relative Humidity,[a] %	Moisture Content, %
1	Offset	47.8	381 x 1270	Baldwin	50	--
2	Bag	52.9	381 x 1270	Baldwin	50	--
2	Bag	52.9	381 x L[c]	Baldwin	50	--
3	Offset	47.8	381 x 2000	LSTT	50	5.7
4	Bond	74.0	381 x 2000	LSTT	50	5.9
4	Bond	--	381 x 2000	LSTT	12 (50)[b]	2.9
4	Bond	--	381 x 2000	LSTT	77 (50)	8.6
4	Bond	--	381 x 2000	LSTT	85 (50)	10.3
4	Bond	--	381 x 2000	LSTT	50 (85)	6.4
5	Kraft	82.5	381 x 2000	LSTT	50 (85)	7.7

[a]All tests at 23°C.

[b]Numbers in parentheses are the relative humidities at which specimens were precon-
ditioned prior to conditioning at the test humidity. All specimens were taken from
rolls in a 50% RH, 23°C atmosphere.

[c]L = variable length.

The specimens were tested as taken from the rolls; i.e., no trimming

or cutting to width was done. However, in the selection of regions of the parent

roll for the cutting of specimens, only those free of edge damage were used.

APPARATUS

The first large-specimen tests were performed on a Baldwin-Southwark testing machine. This very rigid machine was fitted with upper and lower line-type clamps capable of gripping specimens 15 inches in width. The clamps were secured rigidly to the upper and lower crossheads.

In the use of Baldwin testers at low loads (as in this work), strain gages are normally used to measure the applied load. However, our tester is not equipped with this feature, so the loads were measured with the existing hydraulic force balancing system. This hydraulic force balancing system is suitable for the measurement of extremely high loads, but is slow in response. Consequently, the data obtained with the Baldwin tester are most reliable at the higher load levels. Greater uncertainty exists at lower load levels. This uncertainty extends as well to the strain-at-rupture since this value is obtained from the load-elongation plots.

Because of the problems associated with the Baldwin tester, a special apparatus was constructed for the tensile testing of large webs. It is basically a heavy frame arranged for horizontal placement and testing of specimens of up to 24 inches in width and over 10 feet in length. One line-type clamp is driven by a pair of screws rotating at constant speed to provide a constant rate of straining of the specimen. A second clamp is supported by a flex-plate to maintain its alignment parallel with the moving clamp and is attached to a pair of 1000-pound Instron strain gage load cells which straddle the specimen. Half of the strain gage bridge of one cell is coupled to half of the strain gage bridge of the other to form a complete bridge. A balancing potentiometer is inserted in the bridge and adjusted such that the bridge output is independent of the

position of a load along the clamp face. This is desirable since specimens

with edge cracks are not symmetrical about a fixed center line. The force measur-

ing system should not respond to any possible variation in load distribution

across the width of the specimen.

The movable clamp is driven by a variable-speed Graham drive which

was set at a given speed and fixed at that point through the entire testing

program. One of the LSTT drive screws was used to mechanically drive the

elongation axis of the recorder. This ensured that the pen position always

corresponded to a particular position of the movable clamp and removed the

uncertainty of possible small changes in the rate of straining on the results.

RESULTS AND DISCUSSION

CRITICAL STRESS VERSUS INITIAL CUT LENGTH

The most complete and most accurate sets of data were obtained using the newer Large-Specimen Tensile Tester (LSTT). Three different commercial paper samples were evaluated at 50% RH using the LSTT. The results of those evaluations provide a major part of the data base relating tensile strength to initial edge cut length. These data for the web-offset paper, the bond paper, and the kraft paper are summarized in Tables II, III, and IV. Additional data relating to these samples are given in the appendix.

Critical stress values at any test condition are based on the initial cross-sectional area of the specimens, ignoring the presence of the cut. This is conventional practice in fracture mechanics and differs from the usual engineering procedure of computing stress intensification factors on a net-section basis. Although the term "critical stress" is used throughout this report, the values actually given are the product of critical stress, σ_c, and sheet thickness, $\underline{t}$. This product has the units of force per unit width of specimen (newtons/meter).

In comparing the effects of edge cuts on the tensile strengths of different samples, it would be useful if a reference strength value were available for each sample. It would seem that the strength of specimens in which no edge cuts were made would be a good reference value. Unfortunately, this is not the case for two reasons. First, in these large-specimen tests, failure normally originated near the line of clamping, though not at the clamp line. Failures within the central region of the test span were rare. Much attention was given to this matter to check for and eliminate possible instrumental causes, such as poor specimen alignment, inadequate clamping, lack of clamp-line parallelism, etc.

TABLE II

LARGE-SPECIMEN FRACTURE PROPERTIES OF WEB-OFFSET PAPER AT 50% RH

1 Number of Tests	2 Initial Cut Length, a, mm	3 Critical Stress, $\sigma_c t$, N/m	4 Critical Strain, ε_c, %	5 Extensional Stiffness, Et, kN/m	6 $\sigma_c t \sqrt{a}$, N·m$^{-1/2}$	7 $\varepsilon_c \sqrt{a}$, m$^{-1/2} \times 10^4$	8 $\dfrac{(\sigma_c t)^2 \sqrt{a}}{Et}$, N·m$^{-1/2}$	9 Net Section Stress, σ_N, N/m
6	0	2500	1.01	414	--	--	--	2500
6	3.04	1960	0.623	418	108	3.43	0.51	1976
6	4.62	1725	0.505	418	117	3.43	0.48	1746
6	7.48	1380	0.368	418	119	3.18	0.39	1408
6	12.2	1145	0.292	414	126	3.23	0.35	1183
6	24.0	875	0.220	411	136	3.41	0.29	934
6	35.0	795	0.198	408	149	3.70	0.29	875
6	48.0	718	0.183	404	157	4.01	0.28	822
6	70.0	636	0.170	395	168	4.50	0.27	779
6	100.1	571	0.162	367	181	5.13	0.28	775

M.D. Instron   2930   1.51   428

Elastic limit (0.01% strain offset) = 1060 N/m.

TABLE III

LARGE-SPECIMEN FRACTURE PROPERTIES OF BOND PAPER AT 50% RH

1 Number of Tests	2 Initial Cut Length, a, mm	3 Critical Stress, $\sigma_c t$, N/m	4 Critical Strain, ε_c, %	5 Extensional Stiffness, Et, kN/m	6 $\sigma_c t \sqrt{a}$, N·m$^{-1/2}$	7 $\varepsilon_c \sqrt{a}$, m$^{-1/2}$×10^4	8 $\dfrac{(\sigma_c t)^2 \sqrt{a}}{Et}$, N·m$^{-1/2}$	9 Net Section Stress, σ_N, N/m
5	0	3170	0.913	551	--	--	--	3170
4	3.15	2860	0.730	556	161	4.10	0.83	2884
4	4.64	2550	0.599	552	174	4.08	0.80	2581
4	6.15	2320	0.518	556	182	4.06	0.76	2358
4	12.2	1630	0.320	557	180	3.53	0.53	1684
4	24.1	1180	0.222	554	183	3.45	0.39	1260
4	35.0	1010	0.195	535	189	3.65	0.36	1112
4	48.1	885	0.173	541	194	3.79	0.32	1013
4	70.1	772	0.155	516	204	4.10	0.31	946
4	100.1	718	0.153	493	227	4.84	0.33	974

M.D. Instron 3860 1.46 545

Elastic limit (0.01% strain offset) = 1320 N/m.

TABLE IV

LARGE-SPECIMEN FRACTURE PROPERTIES OF KRAFT PAPER AT 50% RH

1 Number of Tests	2 Initial Cut Length, $\underline{a}$, mm	3 Critical Stress, $\sigma_{\underline{c}}t$, N/m	4 Critical Strain, $\varepsilon_{\underline{c}}$, %	5 Extensional Stiffness, $\underline{Et}$, kN/m	6 $\sigma_{\underline{c}}t\sqrt{\underline{a}}$, N·m$^{-1/2}$	7 $\varepsilon_{\underline{c}}\sqrt{\underline{a}}$, m$^{-1/2}$ x10^4	8 $\dfrac{(\sigma_{\underline{c}}t)^2\sqrt{\underline{a}}}{\underline{Et}}$, N·M$^{-1/2}$	9 Net Section Stress, $\sigma_{\underline{N}}$, N/m
6	0	7310	1.475	910	—	—	—	7310
6	3.02	5045	0.755	910	277	4.15	1.54	5085
6	4.44	4350	0.588	910	290	3.92	1.39	4401
6	7.67	3450	0.425	907	302	3.72	1.15	3521
6	12.3	2730	0.315	912	303	3.49	0.91	2821
6	24.0	1920	0.218	905	297	3.38	0.63	2049
6	34.9	1680	0.195	876	314	3.64	0.60	1849
6	48.0	1490	0.175	867	326	3.83	0.56	1705
6	69.9	1290	0.157	841	341	4.15	0.52	1580
6	100.1	1150	0.148	794	364	4.68	0.53	1559
M.D. Instron		9775	2.31	910				

Elastic limit (0.01% strain offset) = 2600 N/m.

No reason could be found for this behavior other than that the normal Poisson contraction of a tensile specimen cannot occur at the clamp line as it will at midspan and that this results in a state of stress at the edges near the clamps which leads to early failure in those regions. It should be noted that in dynamic web transport through converting apparatus, similar behavior may be expected in many instances.

The critical stresses determined for these large uncut specimens were 15, 18, and 25% lower than the average tensile strength of specimens of 1-inch width tested on the Instron apparatus for the web-offset, bond, and kraft papers, respectively. Since the failure of the large uncut specimen originates with a restricted portion of the specimen, weak-link theory should not be applied to explain these differences. The term, Instron tensile strength, refers to the results of tests on specimens of 25.4-mm (1-inch) width.

The second reason for the inadequacy of large uncut specimen strength as a reference strength value lies in the fact that even though no deliberate cuts are made in these large specimens, each has naturally-occurring flaws which act to limit its strength. Though the size of these flaws in not known, they are certainly expected to be different for different papers. Hence, the strength of any uncut sample is itself the consequence of some unknown flaw dimension.

It is useful, nonetheless, to utilize reference strength values of some kind to normalize the critical stress values when first comparing different samples. Chiefly because of its common use in the industry, the Instron tensile strength was employed for this purpose in the presentation of the results shown in Fig. 2. The critical stress at each initial cut length was divided by the Instron tensile strength for that sample and plotted versus the initial cut length. The fact that
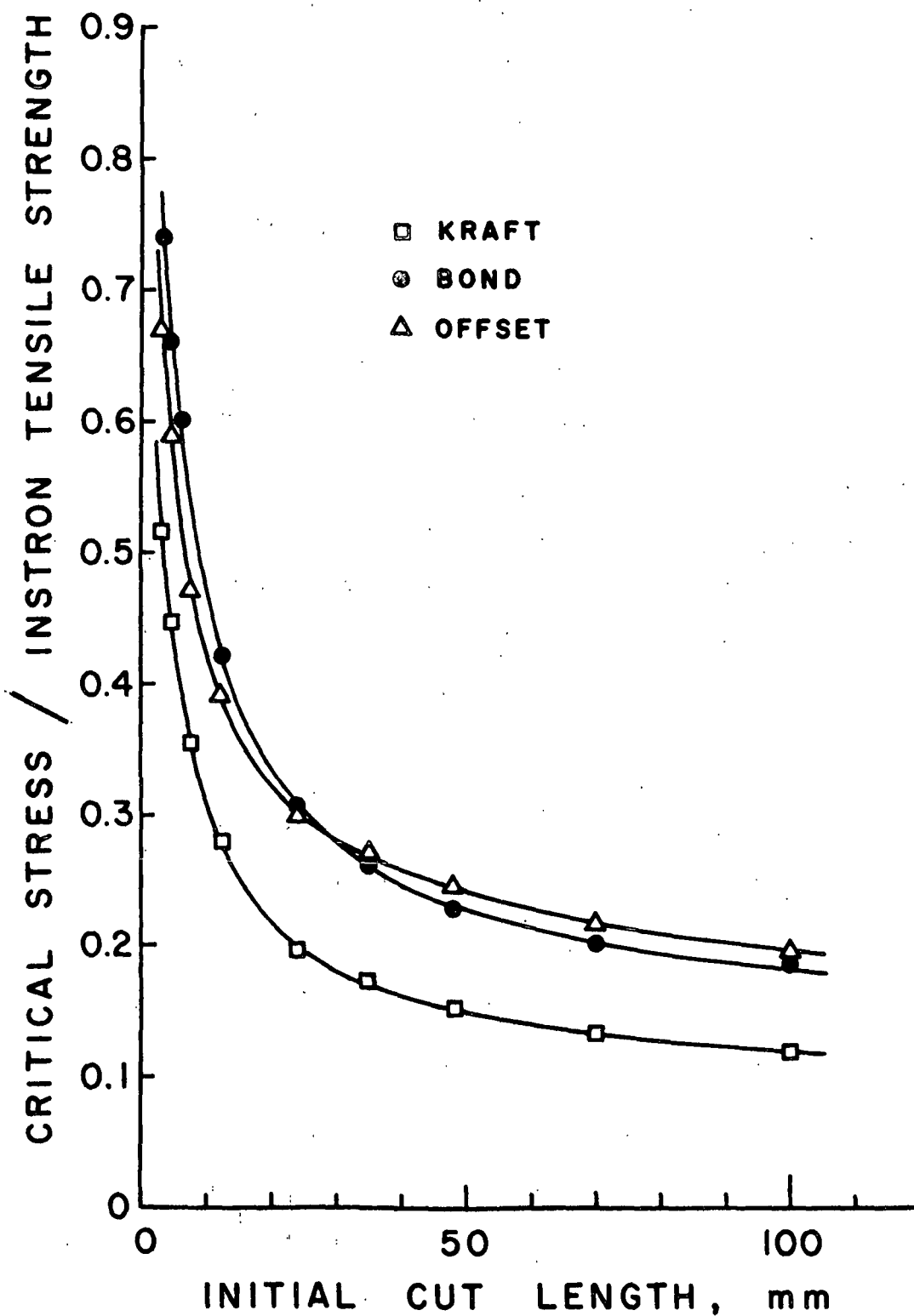
Figure 2. The Effect of Initial Cut Length on the Critical Stress of Three Paper Samples. Critical Stress is Presented as a Fraction of the Instron Tensile Strength for Each Sample. 50% RH

the results for the three samples do not fall on the same curve suggests that the Instron tensile strengths do not properly rate the strength of the samples when flaws of a given size are introduced. Also, the fact that two of the curves cross each other indicates a different response to edge cuts for these two samples.

Curves such as those shown in Fig. 2 illustrate well the very rapid drop in tensile strength which occurs with increasing edge cut length when the edge cuts are small and the rather slow decreases when the edge cut lengths are large. In fact, at the largest edge cuts employed, the stress at rupture tends to approach constancy when computed on the basis of the net or uncut part of the cross-section (σ_n). This indicates that the stress intensification factor is approaching its maximum level at these large cut lengths.

A better way of presenting such data is by a logarithmic plot, as in Fig. 3. For initial cut lengths above 20 mm, the critical stress versus initial cut length data tend to fit a straight line rather well. Of course, the range of each variable is small and other mathematical expressions can also be fitted to these results rather well. For the bond and kraft papers, the slopes above 20-mm cut length are virtually identical at -0.357, whereas a slope of about -0.3 better fits the web-offset paper in this large-cut-length regime. It appears further that for very small initial cut lengths the slopes are about the same, though each curve is displaced upward to critical stresses above those expected by extrapolation of the large-cut-length data.

The critical stresses at the smaller cut lengths are 20 to 25% greater than predicted by the extrapolated large-cut-length data. This increase is very nearly the same for the kraft and bond papers and, in fact, the two curves are
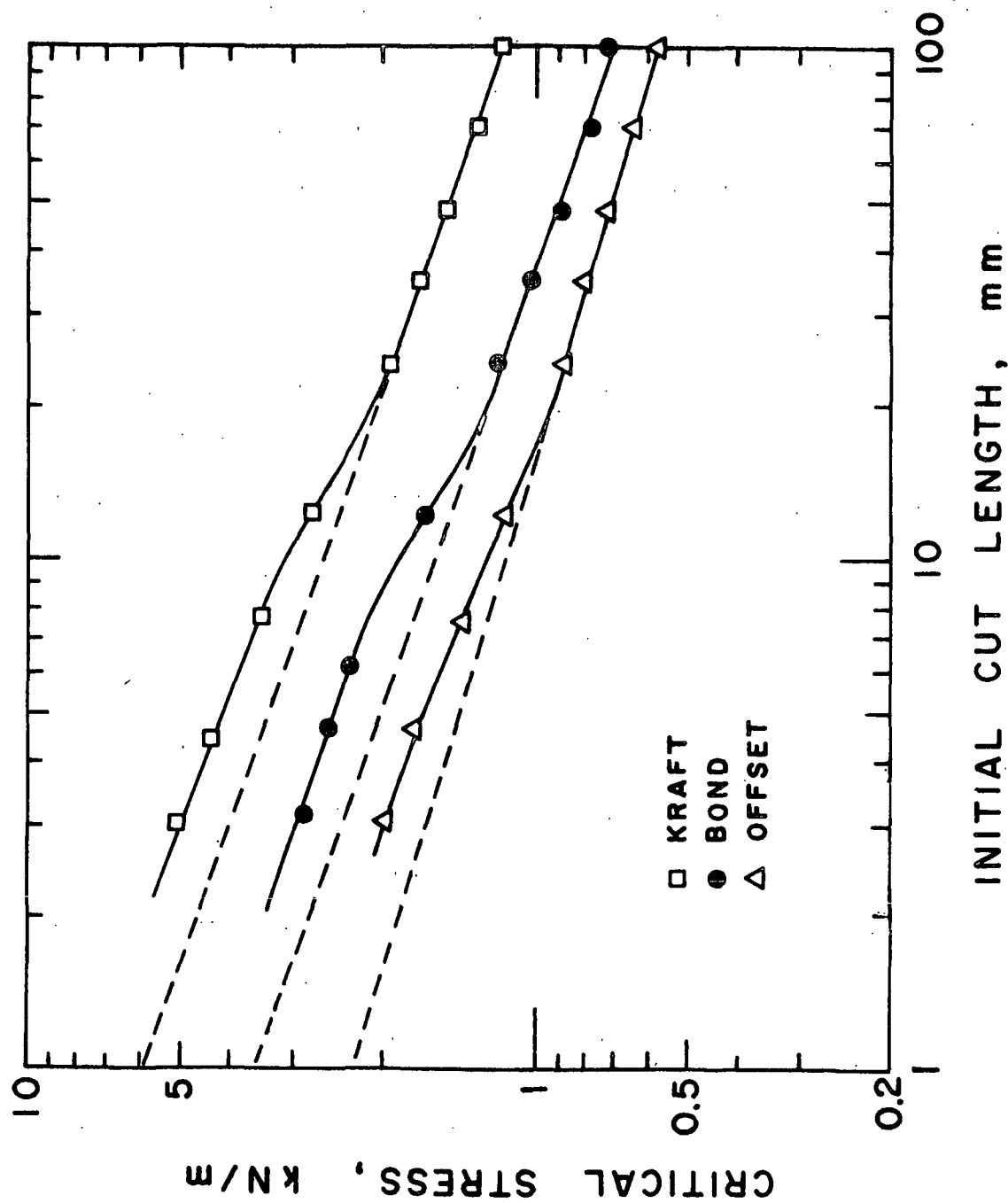
Figure 3. Critical Stress Versus Initial Cut Length for Three Paper Samples
at 50% RH. Logarithmic Plot

practically identical in shape and slope, with the kraft sample shifted upward

to a critcal stress level 1.65 times that of the bond paper at any initial cut

length. Note, however, that the M.D. Instron tensile strength of the kraft

paper is about 2.56 times that of the bond paper at 50% RH. This illustrates

how poor the Instron tensile strength can be in predicting the strength of paper

when edge flaws are present. It is particularly noteworthy that the entire

curve is displaced along the critical stress axis. The rather similar tensile

response to edge cuts of these two samples is striking since they would be

viewed as rather different papers using conventional physical property evaluation

techniques and interpretations.

It is of interest to examine these data with respect to linear elastic

fracture mechanics theory. One recalls, of course, that such theory is applicable

when the specimen is not subjected generally to stresses and strains in excess

of the elastic limit. This means that the tensile stress-strain curves of

specimens containing edge cuts must be linear to the point of incipient fracture.

This condition was met in all three paper samples at initial cut lengths of 24

mm and above. Plots of the critical stresses versus critical strains for all

initial cut lengths for the three samples are given in Fig. 4. The locus of

these points for any sample fits the average stress-strain curve of the sample

quite accurately when the edge cuts are small. The points fall below the stress-

strain curve of an uncut specimen at large initial cut lengths since the apparent

Young's modulus of the cut specimens falls below that of the uncut specimen. In

Fig. 4, the curves quite accurately describe an average stress-strain curve for

each sample. The three points identified by arrows are for initial edge cut

lengths of 12.4 mm. Note that these are about the first points of departure from

Hookian and presumably elastic response. With decreasing initial cut length,
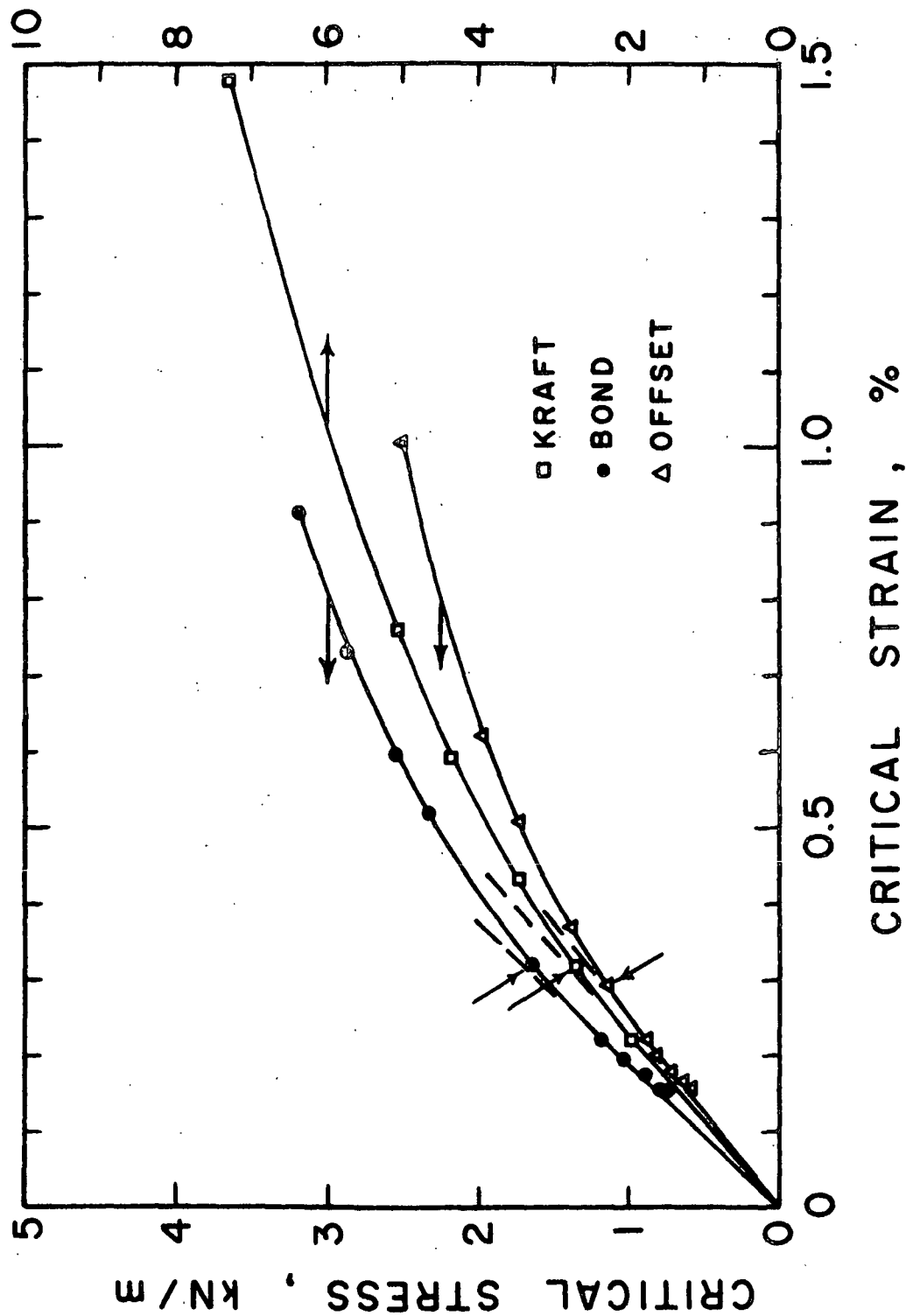
Figure 4. Critical Stress Versus <u>Critical</u> Strain for Three Paper Samples at 50% RH

departure from the linear elastic response becomes greater. The initial cut

length at which the stress-strain curve shows first departure from Hookian re-

sponse is approximately the cut length at which departure also occurs from the

large-cut-length regime as indicated in the logarithmic plot of Figure 3. Thus,

the first departure from Hookian behavior in the tensile fracture of specimens

containing edge cuts could be viewed as the onset of yielding of the specimen,

if one wished to follow this approach in data interpretation.

If linear elastic fracture mechanics (LEFM) theory were directly

applicable to these data, the critical stresses would be proportional to the

initial cut length to the -0.5 power, compared to exponents of -0.357 for two

of the samples and about -0.3 for the other. The unmodified data clearly does

not conform to the expectations of linear elastic fracture theory. However,

a number of considerations must be taken into account before a firm conclusion

is drawn to this effect. These involve crack length corrections and the applica-

tion of correction factors for the finiteness of specimen size.

The first possible problem arises because the length of the cut as

introduced may not properly represent the length of the flaw just prior to

fracture of the specimen. Inspection of the cut tips during loading of the

specimens revealed a small amount of debonding and structural disintegration.

This zone was never very large and only rarely exceeded 1 mm. Such dimensions

are not very important in the large-cut-length regime, where the addition of

2 mm to each initial cut length will have little effect on the results. It

will certainly not bring these data into conformance with LEFM theory.

It is obvious, however, that the application of small, fixed additions

to the initial cut length in the small-cut-length regime can alter the results

considerably. For example, the addition of a fixed crack length increment of
1 mm to each initial cut length value will result in a response in the small-
cut-length regime of approximate constancy in the product of critical stress and
the square root of the modified cut length value. To say that this represents
conformance with LEFM theory would be ludicrous, however, since the specimens
are stressed well beyond the elastic limit.

Finite-Specimen-Size Correction Factors

The basic equations of linear elastic fracture mechanics for Mode I
crack opening (the tensile mode) were developed for specimens of infinite size
containing centrally located cracks oriented perpendicularly to the direction
of applied stress. Real specimens are finite in size and have free surfaces
(edge boundaries). The expected result of both effects is to produce unstable
fracture at nominal tensile stresses below those which would cause fracture in
an infinite specimen. For the linear elastic specimen, the difference in result
due to the specimen size and shape can be calculated. This leads to theoretical
correction factors to be applied to the critical stresses which vary with the
length of the crack and the specimen size. For a given specimen length to width
ratio, the correction factor has particular values at every ratio of edge crack
length, a, to specimen half width, b. It also differs in magnitude for single-
edge-cut and double-edge-cut specimens. Correction factors computed by Bowie
and presented and discussed by Paris and Sih ([9]) are presented in Fig. 5. Be-
cause of differences in nomenclature in the literature and to remove ambiguity
for the reader of this report, the factors are plotted versus the ratio of the
cut length to specimen width, a/w. The correction factors are of similar magnitude
(about 1.12) for small cuts whether present in one or both edges of the specimen.
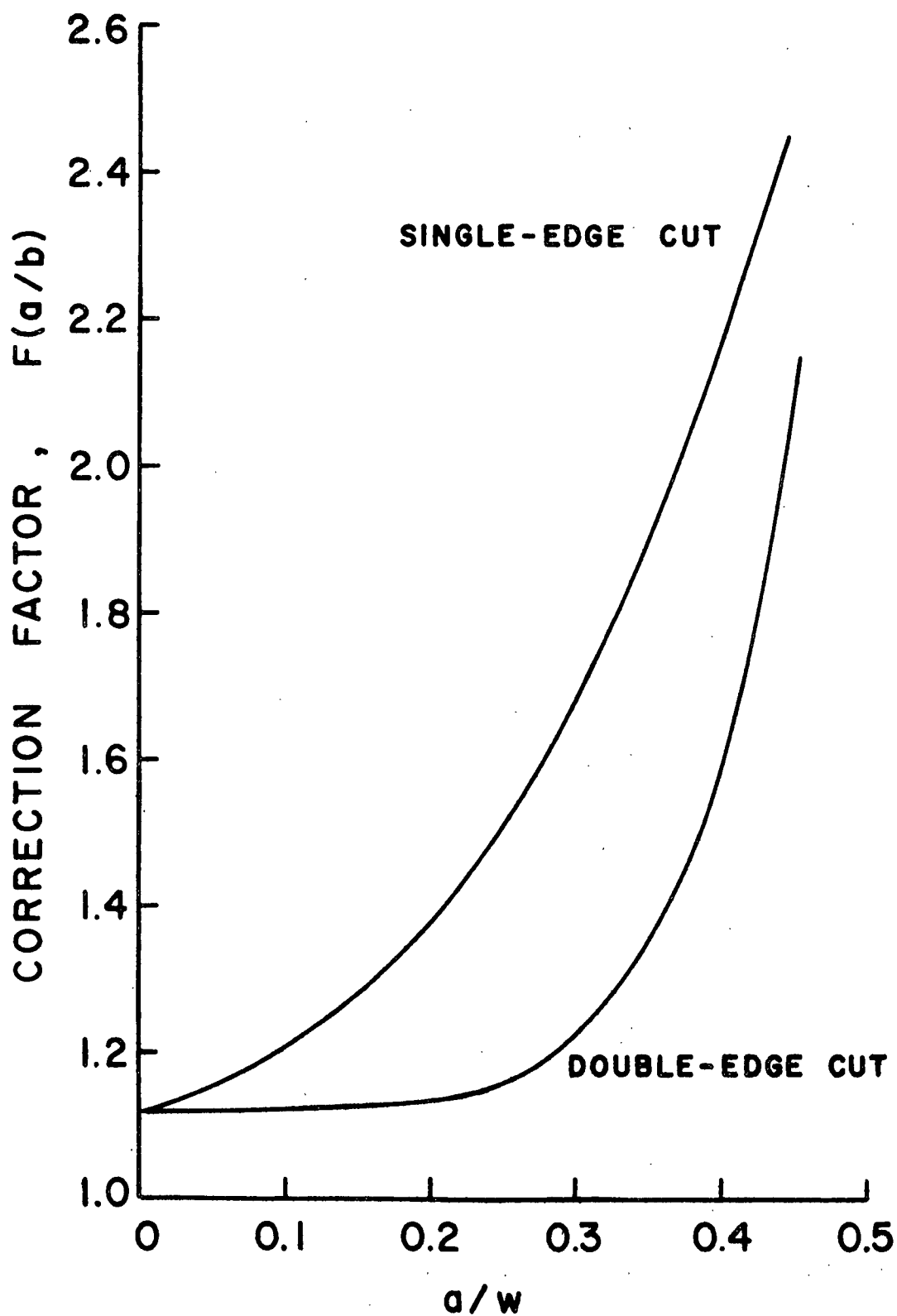
Figure 5. Finite-Specimen-Size Correction Factors for Single-Edge-Cut and Double-Edge-Cut Isotropic Specimens. (L/w) = 3

As the cut length increases, however, the theoretical correction factor increases

much more rapidly for the single-edge-cut specimen.

The need for a means of adjusting the results obtained with single-

edge cuts compared to those obtained with double-edge cuts seems obvious when

one considers the difference in symmetry of loading of these specimens. With

a single-edge cut, there is a tendency for bending about the cut tip which tends

to open the crack and to move the central region of the specimen laterally

(parallel to the clamp line) in the direction of the edge containing the cut.

This should cause a greater intensification of stress at the cut tip and result

in specimen failure at a lower total applied load than in the case of the sym-

metrical double-edge-cut specimens. One should expect these correction factors

to be applicable in practice to isotropic specimens which respond elastically

in their fracture behavior. When this ideal condition is not met, one should

proceed cautiously in the application of these factors.

One possible means of determining whether the theoretical correction

factors are applicable in any particular experimental situation is to change

the system dimensions, then note whether the same results are obtained after

application of the factors. In these large-specimen tests, however, it was not

easy to change the specimen dimensions, nor were correction factors available

for many different geometric shapes. It was possible, however, to hold the

specimen dimensions constant and then to introduce cuts of the same length into

one edge and into both edges of specimens. This was done for the bond paper

at 50% RH using cut lengths of 35 and 70 mm. The results are presented in Table

V. Each value is the average of four tests. Standard errors are in parentheses

following the mean values. In both cases, the critical stress for the single-

edge cut fell slightly below that of the double-edge cut test. However, the

differences between the mean values are not statistically significant. Application of the appropriate $\underline{F}(\underline{a}/\underline{b})$ correction factors made matters worse. It seems apparent from these results that the single-edge-cut correction factors overcorrect and lead to "corrected" critical stresses which are greater than the double-edge-cut values at the 70-mm cut length. If the tests on all the large specimens in this report had been carried out using double-edge rather than single-edge cuts, the results would have been essentially the same, since no difference at all is expected for small cut lengths; and up to 70-mm length, the differences are of minor importance.

<div align="center">TABLE V</div>

<div align="center">CRITICAL STRESSES IN SINGLE- AND DOUBLE-EDGE
CUTS IN BOND PAPER</div>

Cut Length, mm	$\sigma_c \underline{t}$, N/m	$\underline{F}(\underline{a}/\underline{b})$	$(\sigma_c \underline{t})[\underline{F}(\underline{a}/\underline{b})]$, N/m
35 (single)	1010 (19.8)	1.19	1202 (23.6)
35 (double)	1025 (13.1)	1.12	1148 (14.7)
70 (single)	771 (19.9)	1.34	1033 (26.6)
70 (double)	798 (16.9)	1.13	902 (19.1)

0.381 x 2 m specimens tested at 50% RH, 23°C.

It is apparent that no good purpose would be served at this time by applying finite-size specimen correction factors to these data in the large-cut-length regime. That these factors do not apply is not particularly surprising. They are computed on the basis that specimen fracture is in conformance with linear elastic theory. Paper must exhibit a significant nonlinear response in the vicinity of the cut for large cuts and significant inelastic response throughout the entire specimen when the initial cut length is small. Nonlinear

stress-strain response within an appreciable zone in the vicinity of the cut tip

makes the applicability of these theoretical correction factors doubtful.

Plasticity Corrections

Linear elastic fracture mechanics theory has been employed to characterize

successfully the fracture behavior of materials in which an appreciable inelastic

deformation occurs in the region immediately surrounding the crack tip. The term

"plasticity" is applied rather loosely to different kinds and degrees of inelastic

response to stress. One of the simplest plasticity models involves elastic

response up to a particular stress level (the yield stress) after which strain

continues at about that constant yield stress value. The typical stress-strain

curves of paper are quite different. Nonetheless, it may prove useful to examine

the effect of plasticity corrections on the fracture behavior of paper.

Perhaps the simplest plasticity correction involves an estimation of

the size of a plastic region surrounding the crack tip, then adding this di-

mension to the crack length, $\underline{a}$, to obtain a corrected crack dimension, $\underline{a}^*$.

The effective crack tip is then assumed to fall at the boundary between the

plastic and elastically stressed zones. A relationship of the following form

has been proposed for plasticity correction in metals ($\underline{10}$).

$$\Delta a = (1/2)(\sigma_c^2/\sigma_{ys}^2)(a) \tag{5}$$

where

$\Delta \underline{a}$ = crack length correction, m

$\underline{a}$ = crack length, m

σ_c = critical stress, N/m^2

σ_{ys} = yield stress, N/m^2

In employing plasticity corrections of this kind, it is recommended that the critical stress should not exceed 80% of the yield stress. The size of the plastic zone will then be less than 0.32 times the crack length.

The determination of the yield stress can be rather subjective in those cases where the onset of yielding is not very abrupt. For metals, the yield stress often is taken as the point of intersection of the stress-strain curve with a line having the initial slope of the stress-strain curve but offset by 0.2% strain. While useful apparently for metals, this method is of doubtful value for the estimation of a yield stress value for paper.

Rather than select a single yield strength for these paper samples, three values were chosen to determine the effect of the value on the correction which results. The first was close to the point of first departure of the stress-strain curve from its initial straight line. Two higher values were then chosen arbitrarily. The results of making such plasticity corrections are given for the three samples in Tables VI, VII, and VIII. The lower the yield stress used in the computation, the greater the correction; and the greater the correction, the closer is the approach to constancy in the product of critical stress and the square root of the corrected crack length.

The application of plasticity corrections in accordance with Equation (5) does not provide for conformance with the linear elastic fracture mechanics theory even without finite specimen size corrections. An ability to deal properly with nonlinear response and the effect of specimen size is needed, however. Clearly, what is needed is a comprehensive fracture theory which extends from the linear elastic through the plasticity region and embraces all data from the smallest to the largest cut lengths. Attempts to retain the linear elastic

fracture model through the empirical adjustment of one or more parameters may in the final analysis be little more than an empirical representation of the data.

TABLE VI

EFFECT OF PLASTICITY CORRECTIONS TO WEB-OFFSET PAPER

Initial Cut Length, mm	12.2	24.0	35.0	48.0	70.0	100.1
Critical Stress, N/m	1145	875	795	718	636	571
$\sigma_c t\sqrt{a}$, N·m$^{-1/2}$	126.5	135.6	148.7	157.3	168.3	180.7

$\sigma_{ys} t$, N/m	Cut Length Correction, $\Delta a/a$					
1000	0.860	0.383	0.316	0.258	0.202	0.163
1500	0.291	0.170	0.140	0.115	0.090	0.072
2000	0.164	0.096	0.079	0.064	0.051	0.041

$\sigma_{ys} t$, N/m	$\sigma_c t\sqrt{a^*}$, N·m$^{-1/2}$					
1000	172.5	159.4	170.6	176.4	184.5	194.8
1500	143.7	146.6	158.8	166.1	175.7	187.1
2000	136.4	141.9	154.5	162.3	172.5	184.3

Yield stress (0.01% strain offset) = 1060 N/m.
0.381 x 2 m specimens tested at 50% RH, 23°C.

TABLE VII

EFFECT OF PLASTICITY CORRECTIONS TO BOND PAPER

Initial Cut Length, mm	12.2	24.1	35.0	48.1	70.0	100.1
Critical Stress, N/m	1630	1180	1010	885	772	718
$\sigma_c t\sqrt{a}$, N·m$^{-1/2}$	180.0	183.2	189.0	194.1	204.3	227.2

$\sigma_{ys}t$, N/m		Cut Length Correction, $\Delta a/a$				
1200	0.923	0.483	0.354	0.272	0.207	0.179
2000	0.332	0.174	0.128	0.098	0.074	0.064
2800	0.169	0.089	0.065	0.050	0.038	0.033

$\sigma_{ys}t$, N/m		$\sigma_c t\sqrt{a^*}$, N·m$^{-1/2}$				
1200	249.7	223.1	219.9	218.9	224.4	246.7
2000	207.8	198.5	200.7	203.4	211.7	234.4
2800	194.7	191.1	195.0	198.9	208.1	230.9

Yield stress (0.01% strain offset) = 1320 N/m
0.381 x 2 m specimens tested at 50% RH, 23°C.

TABLE VIII

EFFECT OF PLASTICITY CORRECTIONS TO KRAFT PAPER

Initial Cut Length, mm	12.3	24.0	34.9	48.0	69.9	100.0
Critical Stress, N/m	2730	1920	1680	1490	1290	1150
$\sigma_c t \sqrt{a}$, $N \cdot m^{-1/2}$	302.8	297.4	313.8	326.4	341.1	363.7

$\sigma_{ys} t$, N/m			Cut Length Correction, $\Delta a/a$			
2000	0.931	0.461	0.353	0.278	0.208	0.165
3000	0.414	0.205	0.157	0.123	0.092	0.073
4000	0.233	0.115	0.088	0.069	0.052	0.041

$\sigma_{ys} t$, N/m			$\sigma_c t \sqrt{a^*}$, $N \cdot m^{-1/2}$			
2000	420.8	359.5	365.0	369.0	374.9	392.6
3000	360.0	326.5	337.6	346.0	356.5	376.8
4000	336.2	314.1	327.4	337.6	349.8	371.1

Yield stress (0.01% strain offset) = 2600 N/m
0.381 x 2 m specimens tested at 50% RH, 23°C.

CRITICAL STRAIN

In a linear elastic material under load, the stresses and strains are everywhere proportional. In such materials, stress intensification is identical to strain intensification. Hence, the concept that a substance will begin to fracture at some limiting value of intensified stress can be replaced by the concept of fracture initiating at some value of intensified strain. In materials which obey nonlinear stress-strain laws, the two criteria will be different.

Because of the shape of the stress-strain curves of paper, edge cuts have a much greater effect on the critical strain of fracture than on the critical stress (within the small-cut-length regime, of course). This is evident upon inspection of Fig. 4. In fact, the intensification of strain may exceed 6 in these papers and could easily be as much as 10 or even more.

Critical strain is plotted versus initial cut length for the three paper samples in Fig. 6. Several significant differences are noted in these plots compared to the critical stress plots (Fig. 3). First, the data for the kraft and bond papers fit a single curve. The web-offset sample shows lower critical strains in the small-cut-length regime, but not at the longer cut lengths. The differences between the three samples in the large-cut-length regime are really quite small. For the kraft paper in the large-cut-length regime, a slope of -0.28 describes rather well the relationship between log critical strain and log initial cut length.

Within the small-cut-length regime, a slope of -0.62 fits the four points reasonably well for the kraft and bond papers, with a slope of about -0.56 for the web-offset paper.

The product of the critical strain and the square root of the initial cut length is presented in Column 7 of Tables II, III, and IV. This product declines in magnitude with increasing cut length in the small-cut-length regime, only to increase rapidly with increasing cut length in the large-cut-length regime.
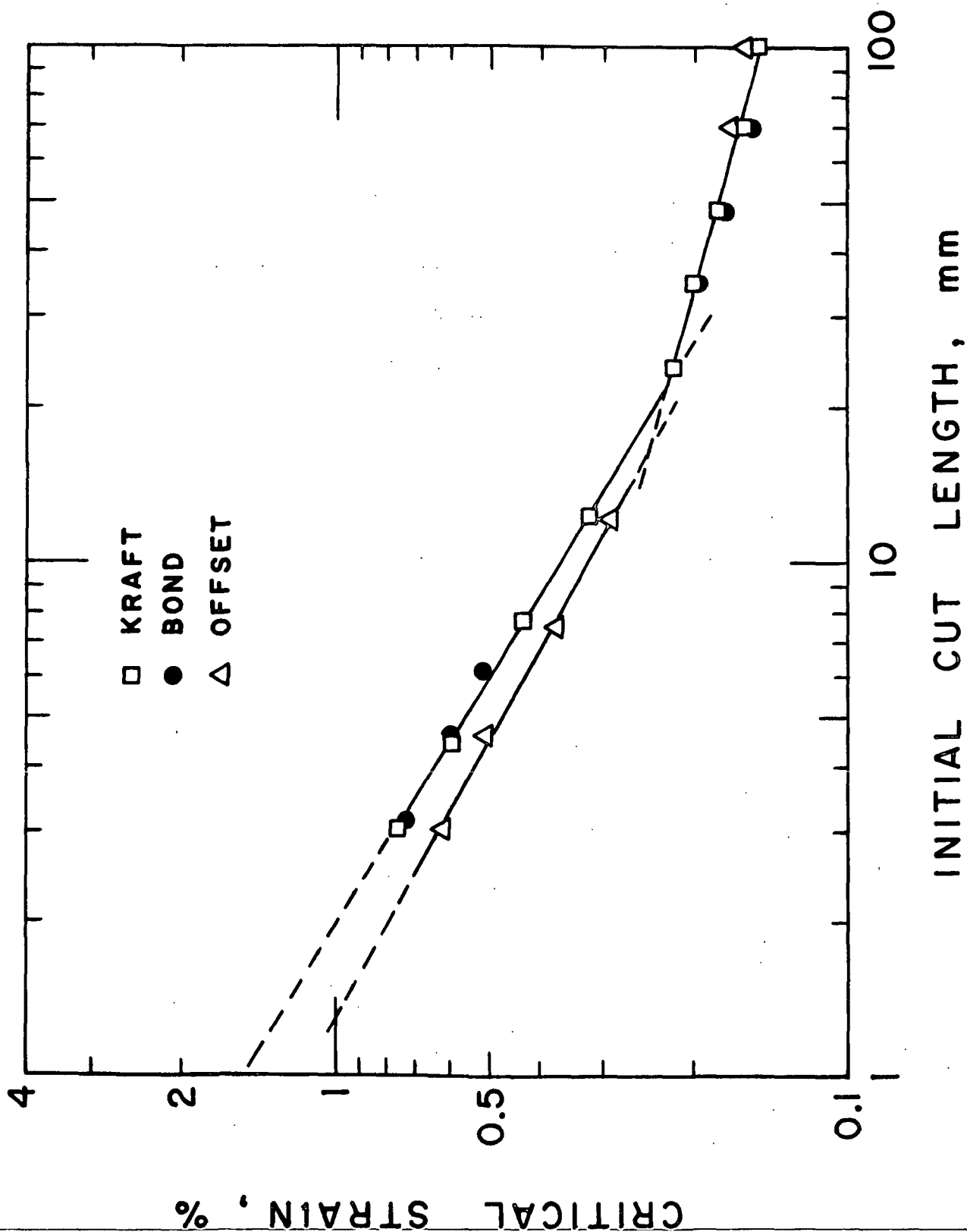
Figure 6. Critical Strain Versus Initial Cut Length for Kraft, Offset, and Bond Papers at 50% RH

STORED ELASTIC ENERGY AT FRACTURE

The total stored elastic energy at the initiation of unstable fracture
cannot be determined accurately if the specimen has experienced a significant
nonlinear, inelastic deformation in the straining period. This will modify the
compliance of the specimen relative to that of the initial loading period.
Though such data are not available, it is possible to estimate the stored elastic
energy based on the initial compliance. This stored energy is proportional to
$(\sigma_c t)^2/Et$. This term multiplied by $(a)^{1/2}$ is given in Column 8 of Tables II,
III, and IV. It may be seen that this product tends to approach a constant value
at the largest initial cut lengths, but is different in magnitude for each sample.
This is an interesting empirical observation which has been of little value thus
far in the interpretation of these results.

THE EFFECT OF MOISTURE CONTENT

Changes in the moisture content of paper are, in principle if not in
practice, one of the simplest means of altering the mechanical properties of
paper. The effect of moisture content on many paper properties is quite well
known. For example, increasing moisture content is expected to result in lower
tensile strengths and increased stretch (elongation at rupture). The tearing
strength is expected to increase with increasing moisture content, but if the
moisture content is too high, the tearing strength may then decrease. From the
standpoint of the fracture behavior of large specimens containing edge flaws,
changes in bonding strength, in the energy needed to propagate a fracture, and
in the stress-strain response are all of interest. The purpose of these experi-
ments was to help understand the phenomena of large-specimen fracture and only
secondarily to develop some insight into how an optimum moisture content can be
established at which maximum resistance to web breaks in use can be expected.

The results of tests performed at 12, 77, 50 (85), and 85% RH on bond paper are presented in Table IX through XII. Data for the 50% RH condition were given earlier in Table III.

Critical Stress

The critical stresses are plotted versus initial cut length in Fig. 7. The changes in moisture content resulted in rather different responses within the small-cut-length and large-cut-length regimes. For example, in tests at 12% RH the critical stresses at small cut lengths were virtually the same as those at 50% RH, whereas at large-cut lengths the critical stresses at 12% RH fell below those at 50% RH (also below those obtained at 77% RH). This rather important observation needs some explanation. It supports the view that there are two different regimes of fracture response which appear distinctly for many paper samples and environmental test conditions. This means that, knowing only a critical stress at one cut length in the large-cut-length regime, one might estimate other data points within that regime with some reliability, but might not predict critical stresses in the small-cut-length regime with any confidence. One should allow for the possibility that papers can be produced which will have the critical stress versus cut length behavior of the bond paper at 77% RH, but at lower relative humidities.

The transition region between the small-cut and large-cut regimes generally corresponds to the change from principally elastic to increasingly inelastic behavior. However, in this series of tests, the transition region virtually disappears in the data obtained at 77% and 85% relative humidity, although in the latter case only three points are available for analysis.

TABLE IX

LARGE-SPECIMEN FRACTURE PROPERTIES OF BOND PAPER AT 12% RH

1	2	3	4	5	6	7	8	9
Number of Tests	Initial Cut Length, a, mm	Critical Stress, $\sigma_c t$, N/m	Critical Strain, ε_c, %	Extensional Stiffness, Et, kN/m	$\sigma_c t\sqrt{a}$, N·m$^{-1/2}$	$\varepsilon_c\sqrt{a}$, m$^{-1/2}$ x10^4	$\dfrac{(\sigma_c t)^2\sqrt{a}}{Et}$, N·m$^{-1/2}$	Net Section Stress, σ_N, N/m
6	0	3480	0.721	603	--	--	--	3480
4	3.27	2910	0.559	600	166	3.20	0.81	2935
4	4.71	2580	0.480	597	177	3.29	0.77	2612
4	6.10	2280	0.406	603	178	3.17	0.67	2317
4	12.4	1630	0.278	598	182	3.10	0.49	1685
4	24.2	1040	0.176	592	162	2.74	0.28	1111
4	35.2	902	0.156	583	169	2.93	0.26	994
4	48.2	792	0.139	582	174	3.05	0.24	907
4	70.4	735	0.132	559	195	3.50	0.26	902
4	100.1	643	0.124	531	203	3.92	0.25	872

M.D. Instron   4424   1.14   618

Elastic limit (0.01% strain offset) = 1770 N/m.

TABLE X

LARGE-SPECIMEN FRACTURE PROPERTIES OF BOND PAPER AT 50% RH
(SPECIMENS PRECONDITIONED AT 85% RH)

1	2	3	4	5	6	7	8	9
Number of Tests	Initial Cut Length, $\underline{a}$, mm	Critical Stress, $\sigma_c \underline{t}$, N/m	Critical Strain, $\varepsilon_{\underline{c}}$, %	Extensional Stiffness, $\underline{Et}$, kN/m	$\sigma_{\underline{c}} t \sqrt{\underline{a}}$, N·m$^{-1/2}$	$\varepsilon_{\underline{c}} \sqrt{\underline{a}}$, m$^{-1/2}$ x10^4	$\dfrac{(\sigma_{\underline{c}} \underline{t})^2 \sqrt{\underline{a}}}{\underline{Et}}$, N·m$^{-1/2}$	Net Section Stress, $\sigma_{\underline{N}}$, N/m
6	0	3009	1.01	509	—	—	—	3009
6	3.31	2700	0.82	513	155	4.79	0.82	2724
6	12.4	1673	0.379	504	186	4.22	0.62	1729
6	48.3	934	0.195	500	205	4.29	0.38	1070
M.D. Instron		3675	1.50	519				

Elastic limit (0.01% strain offset) = 1200 N/m.

TABLE XI

LARGE-SPECIMEN FRACTURE PROPERTIES OF BOND PAPER AT 77% RH

1	2	3	4	5	6	7	8	9
Number of Tests	Initial Cut Length, $\underline{a}$, mm	Critical Stress, $\sigma_c \underline{t}$, N/m	Critical Strain, ε_c, %	Extensional Stiffness, $E\underline{t}$, kN/m	$\sigma_c \underline{t}\sqrt{\underline{a}}$, N·m$^{-1/2}$	$\varepsilon_c \sqrt{\underline{a}}$, m$^{-1/2}$ ×10^4	$\dfrac{(\sigma_c \underline{t})^2 \sqrt{\underline{a}}}{E\underline{t}}$, N·m$^{-1/2}$	Net Section Stress, σ_N, N/m
6	0	2405	1.208	435	—	—	—	2405
4	3.32	2095	0.917	433	121	5.28	0.58	2113
4	4.53	1990	0.820	440	134	5.52	0.61	2014
4	6.18	1730	0.628	434	136	4.86	0.54	1759
4	12.2	1420	0.425	439	157	4.69	0.51	1467
4	24.1	1115	0.299	439	173	4.64	0.44	1190
4	35.2	960	0.256	428	180	4.80	0.40	1058
4	48.1	860	0.226	428	189	4.96	0.38	984
4	70.3	782	—	412	207	—	0.39	959
4	100.2	665	—	398	211	—	0.35	902

M.D. Instron   2960   1.62   430

Elastic limit (0.01% strain offset) = 850 N/m.

TABLE XII

LARGE-SPECIMEN FRACTURE PROPERTIES OF BOND PAPER AT 85% RH

1	2	3	4	5	6	7	8	9
Number of Tests	Initial Cut Length, $\underline{a}$, mm	Critical Stress, $\sigma_{\underline{c}}\underline{t}$, N/m	Critical Strain, $\varepsilon_{\underline{c}}$, %	Extensional Stiffness, Et, kN/m	$\sigma_{\underline{c}}\underline{t}\sqrt{\underline{a}}$, N·m$^{-1/2}$	$\varepsilon_{\underline{c}}\sqrt{\underline{a}}$, m$^{-1/2}$×10^4	$\dfrac{(\sigma_{\underline{c}}\underline{t})^2\sqrt{\underline{a}}}{Et}$, N·m$^{-1/2}$	Net Section Stress, $\sigma_{\underline{N}}$, N/m
6	0	1924	1.24	365	--	--	--	--
4	3.33	1750	1.02	364	101	5.89	0.49	1765
4	12.4	1205	0.50	361	134	5.57	0.45	1246
4	48.3	775	0.26	364	170	5.71	0.36	888
M.D. Instron		2435	1.61	412				

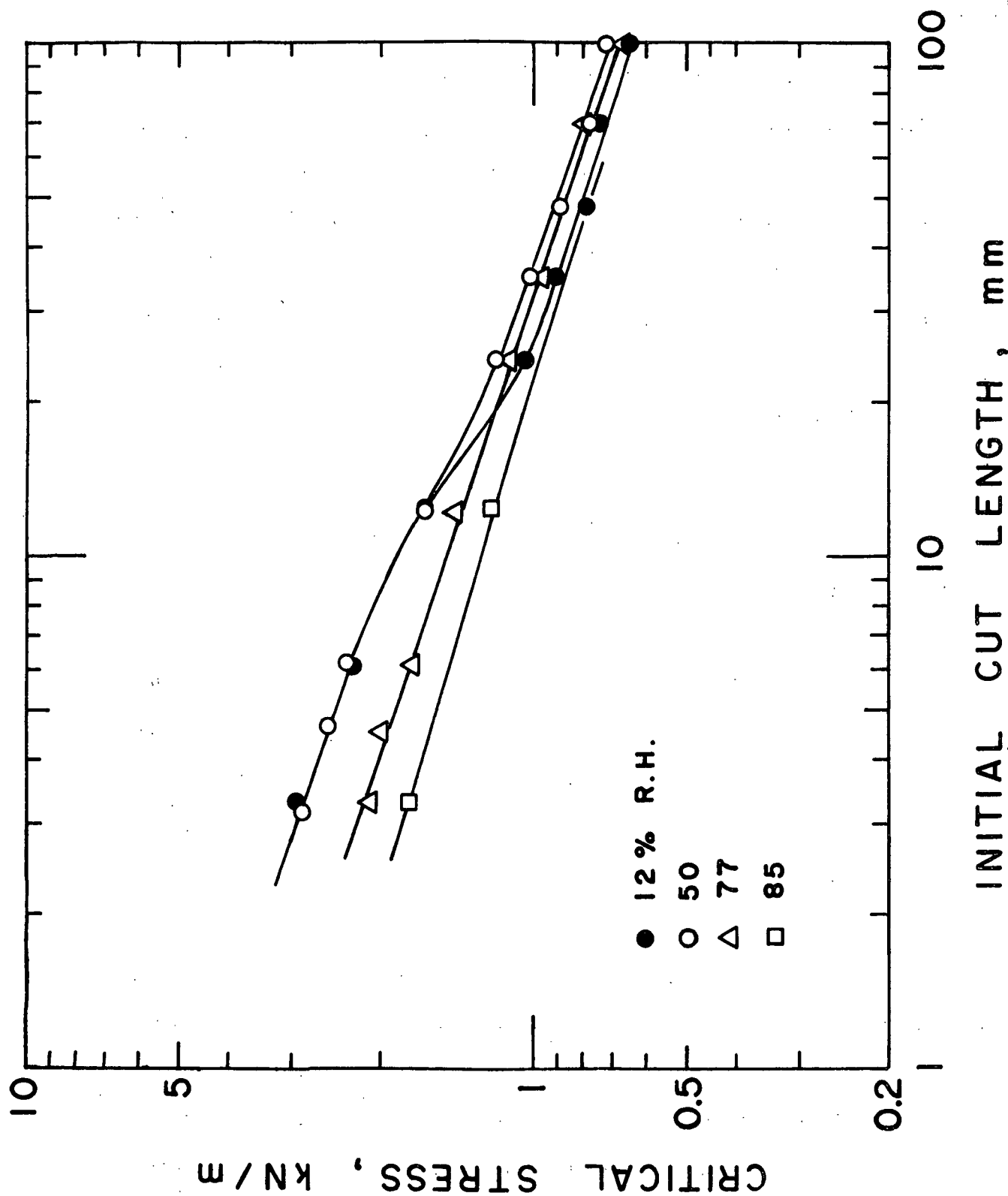Elastic limit (0.01% strain offset) = 600 N/m.

Figure 7. Critical Stress Versus Initial Cut Length for the Bond Paper
at Different Relative Humidities

Critical Strain

The critical strains are plotted versus initial cut length for the bond
paper specimens tested at the different relative humidities in Fig. 8. In the
tests at the two highest relative humidities, at the longest cut lengths, one
can observe slow crack growth. The stress-strain curve shows some "noise" typical
of stable tearing for a short period of time; this is followed quickly, however,
by unstable fracture. It is difficult when this occurs to establish a proper
critical strain value. When the accuracy of the critical strain value was in
doubt, it was not recorded.

Because of the similarity in curve shapes in Fig. 8, all were drawn
such that the effect of changing moisture content could be accounted for simply
by shifting a single curve along the critical strain axis. The critical strain
is the total strain to the point of unstable fracture and includes both the
elastic and inelastic deformation. This is a most interesting result because
of the potential simple means it offers in relating the small-cut and large-cut
regimes. When viewed in terms of the bond paper tested at different moisture
contents, there is no problem. Interestingly, the relationship shown in Fig. 8
also applied to the kraft paper, but not to the web-offset paper (see Fig. 6).
The slope of the critical strain versus initial cut length relationship on the
logarithmic plot of Fig. 8 is approximately -0.58 in the small-cut-length regime.
That a similar value applies to all of the small-cut-length data over a range
of 12 to 85% RH is particularly surprising since the critical strain was much
less elastic at the higher relative humidities. At the 3.33-mm cut length,
the critical strain was about 87% elastic (computed) in tests at 12% RH versus
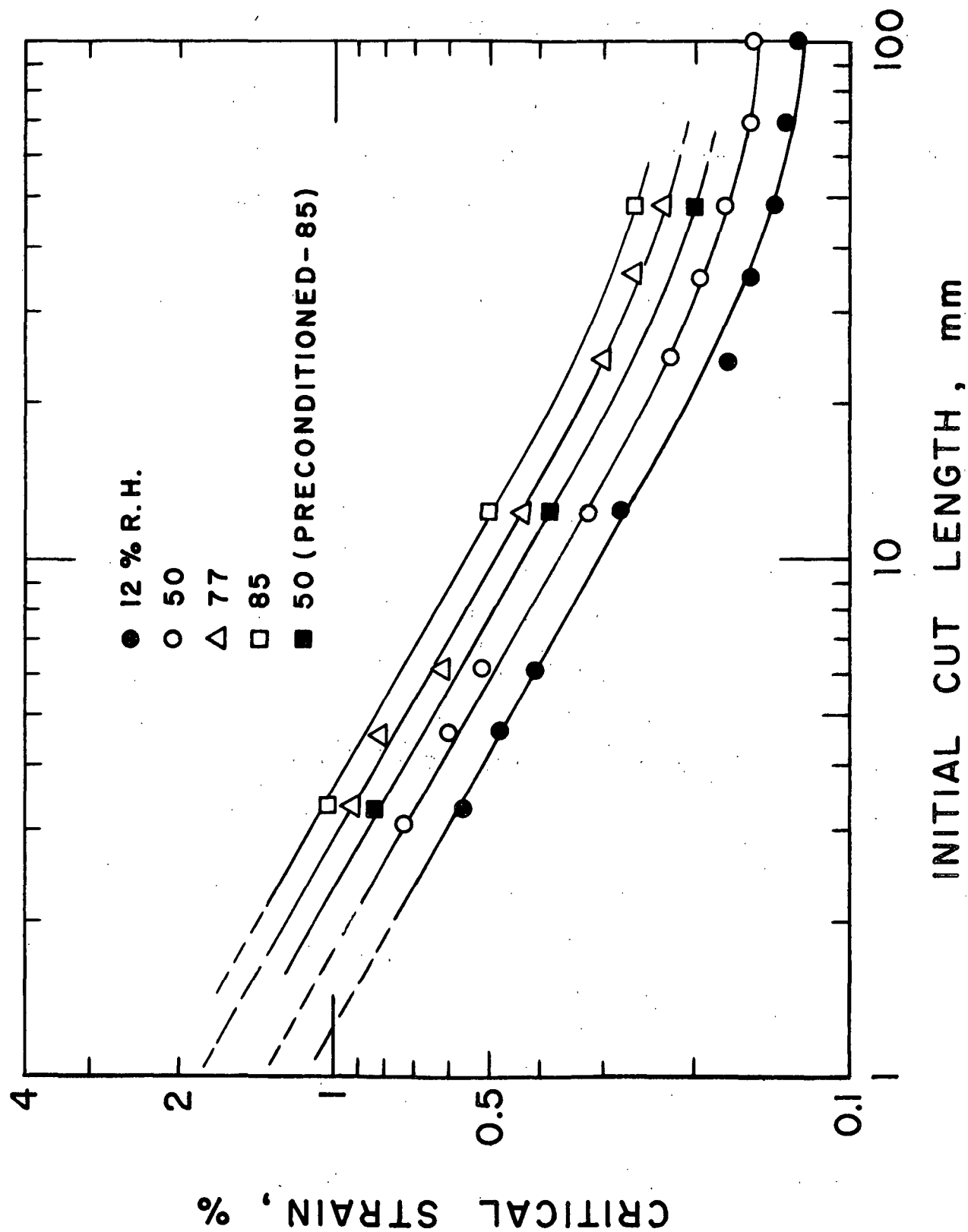only 53% elastic at 77% RH.

Figure 8. Critical Strain Versus Initial Cut Length for Bond Paper at Various Relative Humidities

CORRELATIONS BETWEEN CRITICAL STRESS AND PAPER PROPERTIES

An examination of the change in physical properties of the bond paper
with changing moisture content (Table XX, appendix) suggests that the low criti-
cal stress at 12% RH and large cut lengths might be related to the low cross-
machine direction (C.D.) in-plane tearing strength at that relative humidity.
The logic of such a relationship arises in the expectation that a characteristic
energy release rate should characterize the fracture behavior of a particular
paper at large cut lengths. An energy release rate value might also be expected
to correlate reasonably well with the C.D. in-plane tearing strength (4).

Problems in applying finite-size correction factors to these data,
plus the even greater uncertainty about applying arbitrary plasticity correc-
tions, raise serious questions about the validity of stress intensity factors
and energy release rates based on modifications of linear elastic fracture theory.
To seek correlations between large-specimen fracture behavior and various physical
properties determined on small specimens is warranted, however. From simple LEFM
theory, the critical energy release rate, G_c, is related to the critical stress
for isotropic substances as shown earlier in Equation (4). Assuming that the
energy release rate is proportional to the C.D. in-plane tearing strength and
using the M.D. extensional stiffness, Et_{md}, in place of the Young's modulus of
an isotropic body, a relationship of the following kind might be expected.

$$(U_{cd} \, Et_{md})^{1/2} = B(\sigma_c t)_a \qquad (6)$$

where

U_{cd} = in-plane tearing strength, cross-direction, N

Et_{md} = extensional stiffness, machine-direction, N/m

$(\sigma_c t)_a$ = critical stress at initial cut length, a, N/m

B = constant of proportionality, $m^{-1/2}$

A plot of the left side of the above equation <u>versus</u> the critical stress at an initial cut length of 48.3 mm is shown in Fig. 9. This is only a fair correlation, which may have some value since the extensional stiffness and in-plane tear data are easily acquired. The error in the critical stress estimate would not be serious if it were no worse than that shown in Fig. 9. However, even if one were able to predict the critical stress level at any particular cut length in the large-cut-length regime, this does not enable one to predict the critical stress level in the small-cut-length regime where web runnability may be determined.

The ratio of the critical stress at a cut length of 3.33 mm (a somewhat larger cut length would work equally well) to the critical stress at 48.3 mm is a fair measure of the difficulty of predicting critical stresses at a small cut length from a value at a given large cut length. These ratios varied from 2.25 at 85% RH to about 3.7 in tests at 12% RH, and from 3.25 for the kraft paper to 2.65 for the web-offset paper in tests at 50% RH. In a rather general way, it was noted that the highest ratios occurred in samples having high M.D. elastic moduli relative to their C.D. in-plane tearing strengths. This observation led to a check of a correlation which is always of interest in the study of materials: namely, that between elastic moduli and strength.

A plot of the critical stress at 3.33-mm initial cut length <u>versus</u> the M.D. extensional stiffness for all sample sets showed a fair degree of correlation between these two parameters. However, differences in the C.D. in-plane tear strength had a small effect on the critical stress at this cut length. The in-plane tear strength was then taken into account, giving the following empirical relationship.
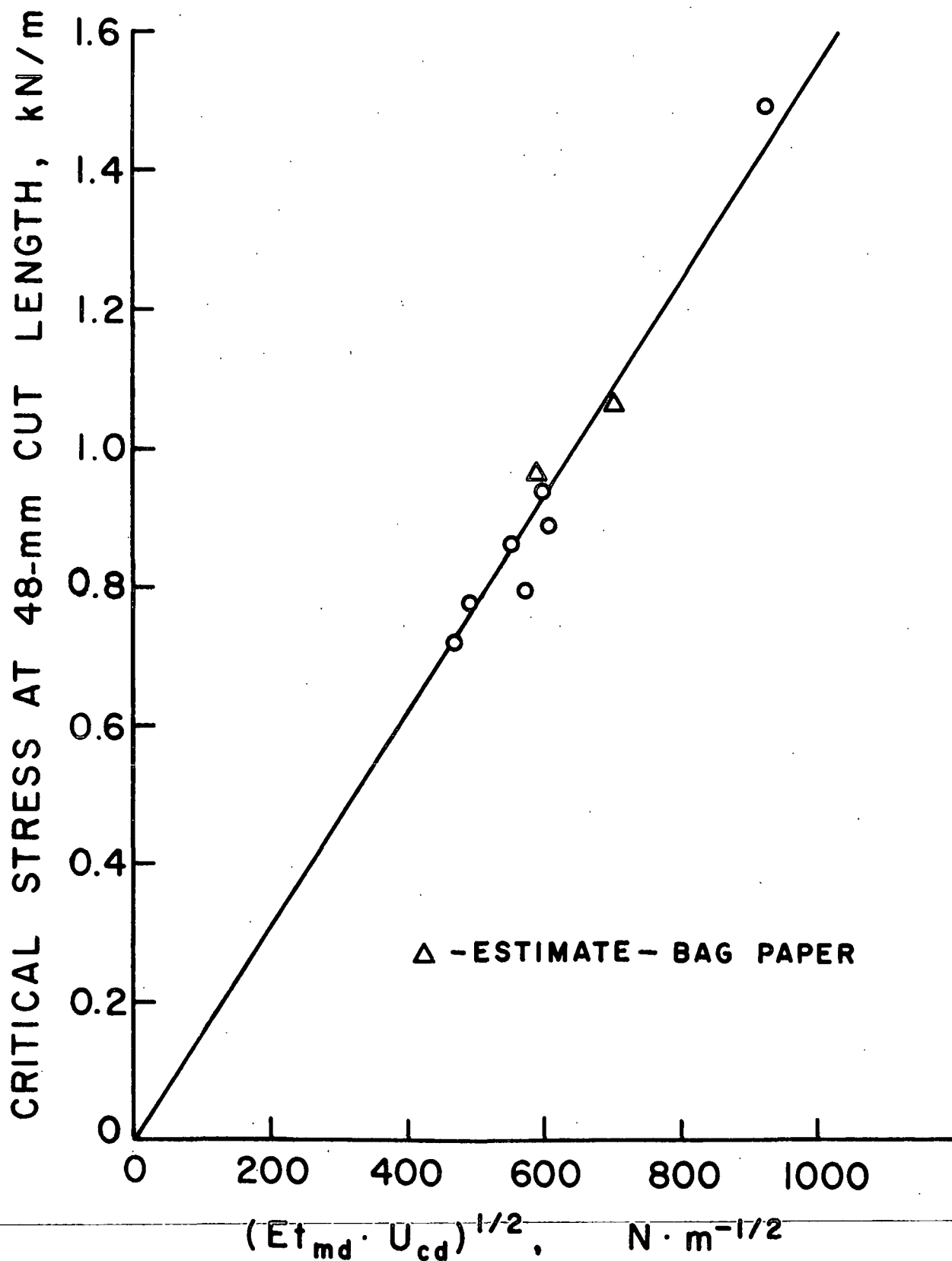
Figure 9. Critical Stress at 48.3-mm Initial Cut Length <u>Versus</u> the Square Root
of the Product of the M.D. Extensional Stiffness and the C.D.
In-plane Tearing Strength for the Bond Paper

$$(\sigma_c t)_{3.33} = 5.46 \, Et_{md} \, U_{cd}^{0.233} \tag{7}$$

The result is an excellent empirical correlation (see Fig. 10) in which the critical stress at 3.33 mm depends rather strongly on the M.D. extensional stiffness and weakly on the C.D. in-plane tearing strength. All values in Equation (7) are expressed in units of newtons and meters. The M.D. extensional stiffness to C.D. in-plane tearing strength ratios varied by about 2.5 to 1 for this array of samples.

It was noted that the correlation between the Instron M.D. tensile strength and the M.D. extensional stiffness was not very good. The Instron tensile strength is a function of the size of the naturally-occurring flaws in the specimens, whereas the elastic modulus (extensional stiffness) is quite insensitive to the presence of a single flaw of critical size. When the flaw size is adjusted to the same small value in all samples, the correlation improves. The simple correlation of Equation (7) deserves further study to establish its general applicability or lack of same using a wider array of samples than have been tested thus far. It is an extremely interesting result which could do much to enhance the value of elastic modulus and in-plane tearing strength data in routine paper evaluation.

Having an ability to estimate a critical stress in large specimen tests at one small and one large cut length is quite helpful at this stage of development of the subject, but it does not solve the problem of characterizing paper fracture behavior. Consider that a flaw of 10-mm length at the edge of the web may be of principal interest in web runnability. This cut length falls within the transitional range (see Fig. 3 and 7). Presumably one could develop correlations at any initial cut length, taking into account that, as the cut
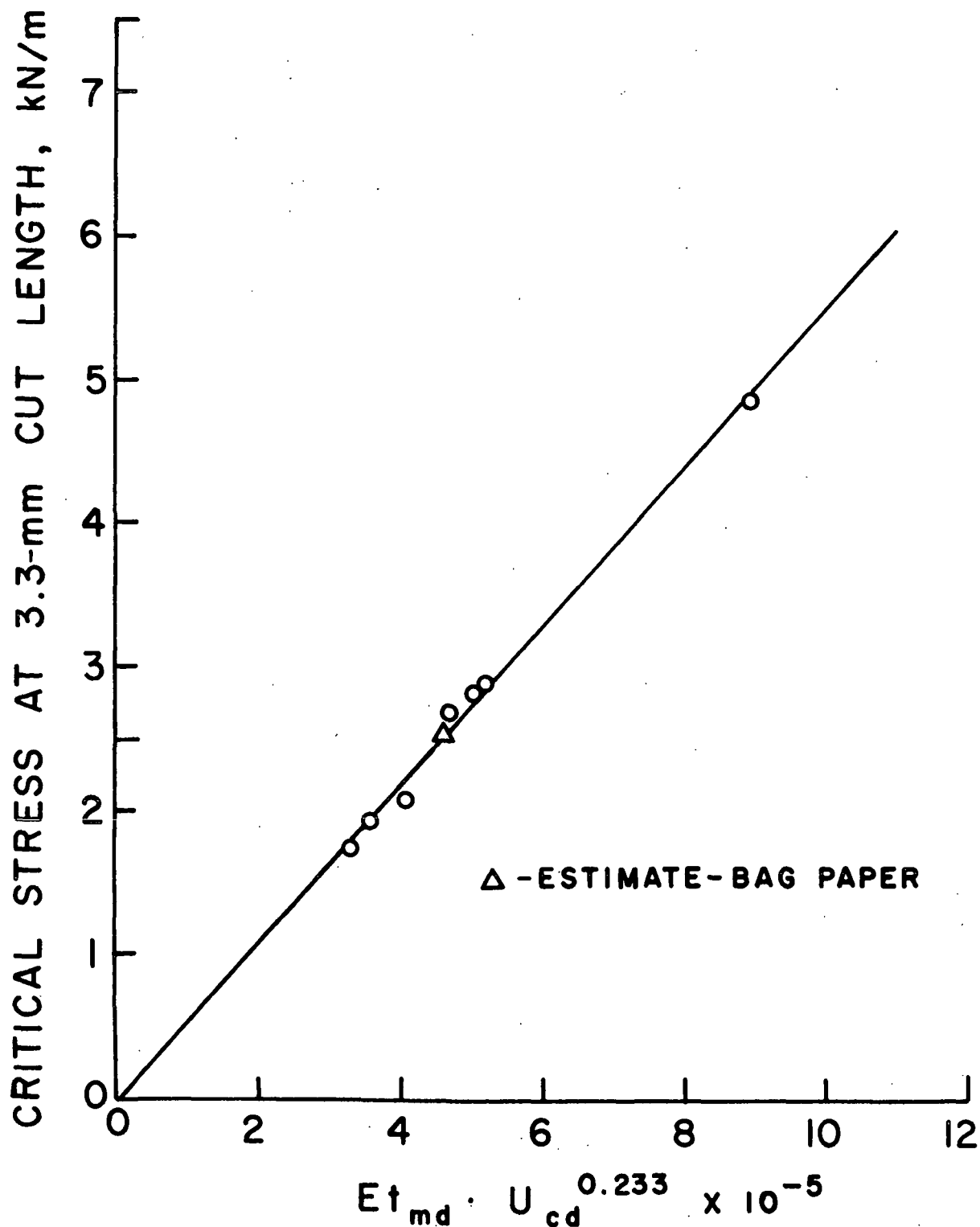
Figure 10. Correlation Between Critical Stress at 3.3-mm Initial Cut
Length and $Et_{md} \cdot U_{cd}^{0.233}$ for the Bond Paper

length increases, the critical stress becomes increasingly dependent on the
tearing energy term. What is needed and what will ultimately be developed in
place of empirical correlations is a practical fracture theory which extends
over the entire range of initial cut lengths and which takes into proper account
the stress-strain law of the material. In this respect, paper might best fit
the model of a brittle material, but one which is not linearly elastic. In view
of the kind of stress-strain curve one usually sees in commercial papers in the
machine direction, a nonlinear elastic model should be far superior to the plasticity
correction approach.

STRAIN ALLOWANCE ANALYSIS FOR RUNNABILITY OF PAPER WEBS

Before a choice can be made of the conditions in the manufacture of
paper to obtain best runnability at any flaw dimension, one needs to know a great
deal about the operation of converting apparatus. One can, of course, reduce
the frequency of web breaks for any given paper by imposing lower stresses and
strains on the web in the converting operation. There are, presumably, valid
requirements of stress or strain which should be met for best operation. Web
tension arises because the web drives portions of the apparatus, because of
frictional drags which may be present, and because of the need to pull the web
free of surfaces to which it tends to adhere (inked rolls or plates, adhesive
coated rolls, etc.). A minimum tension might be needed for proper web guiding.
On the other hand, there are variations in web strain which arise because of
changes in the speed of different sections of the machine and because of roll
eccentricity, including the paper rolls.

Figure 11 was prepared by plotting the critical stress versus the
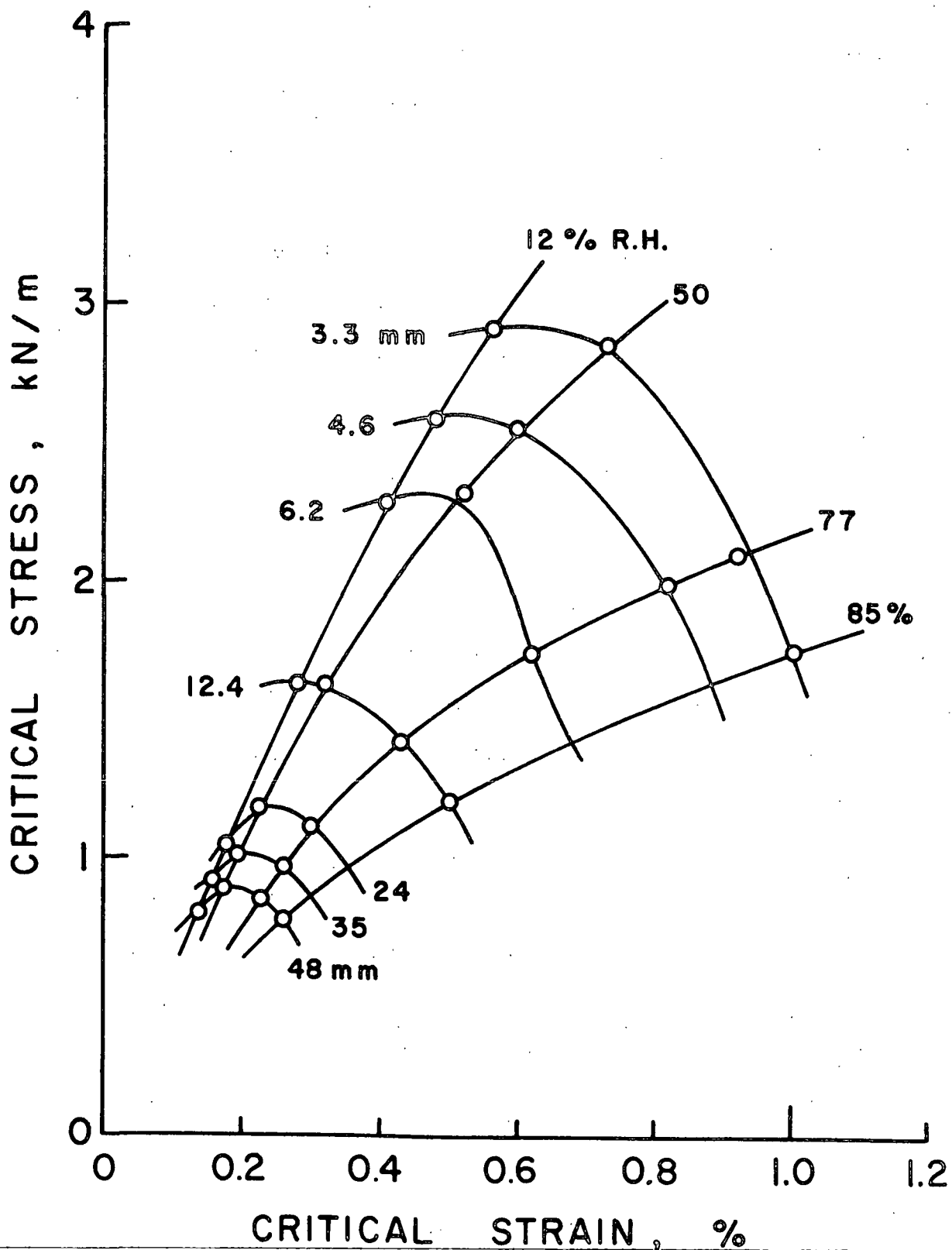critical strain for four different moisture conditions and various edge cut

Figure 11.   Plot of Critical Stress, Critical Strain, Initial Cut Length,
and Moisture Content for Bond Paper

lengths. It is immediately apparent that there are disadvantages in supplying paper at the very low moisture content of 2.9% (in equilibrium with 12% RH). The strength of the dry sheet in the small-cut-length regime is about the same as at 50% RH (5.9% moisture content), but the critical strain is appreciably lower leaving little margin for strain fluctuations. As the moisture content is raised further, a drop in strength occurs with a gain in the critical strain. The effect of increasing moisture content on runnability is not obvious.

Assume that one needed to operate a converting apparatus with a web tension of 1000 N/m and that occasional large flaws at the edge of the web are the equivalent of 12.4-mm edge cuts. The web strains will fall within the Hookian region of response at 1000 N/m tension except for the sample at 77% RH, where a small inelastic strain component will be present at this stress level. The difference between the expected operating strain and the critical strain at 12.4-mm cut length gives the additional strain (strain allowance) which may develop before fracture will occur (see Table XIII).

TABLE XIII

ANALYSIS OF STRAIN ALLOWANCE IN RUNNABILITY

Test Condition, % RH	E_t, kN/m	Operating Strain, %	Critical Strain, %	Strain Allowance, %
12	600	0.17	0.28	0.11
50	555	0.18	0.32	0.14
77	435	0.25	0.43	0.18
50 (85)	510	0.20	0.38	0.18

Bond paper.
1000 N/m stress.
0.381 x 2.0 m specimens.
12.4-mm single-edge cut.

The strain allowance in this example was 0.14% at the 50% RH condition
compared to only 0.11% at 12% RH. A larger strain allowance occurs at 77% RH but
at the expense of operating with some inelastic straining of the sheet. The
better condition appears to be the sheet which was preconditioned at 85% RH and
then reconditioned at 50% RH before testing at 50% RH. That sheet retained its
strength in the presence of small edge cuts and gained in critical strain as
well. It is preferred in this example because of its higher elastic modulus
and yield stress. Sheets having this quality can presumably be made by drying
under less machine-direction restraint. The computation of strain allowances
is suggested for comparison of the runnability quality of different papers.

THE FRACTURE PROPERTIES OF BAG PAPER

Prior to the construction of the LSTT apparatus, large-specimen fracture
tests were carried out on the Baldwin tester using specimens 0.381 x 1.27 m in
size. Two different samples were evaluated: a web-fed offset sample taken from
the same parent roll as the sample set tested later on the LSTT and a lightweight
bag paper. The results obtained on the web-offset paper on the two testers agreed
quite well. The small differences could have been due to differences in the sample
sets used; the results are not given, therefore, in this report. The bag paper,
however, was of particular interest because of its rather high tearing strength
compared to its tensile strength. This sample posed a number of severe problems
in evaluation, however. It was a rather poorly formed sheet compared to the
others, which may explain the greater variability between tests. However, the
major problem was the extreme difference in properties across the width of the
narrow 0.381-m (15-inch) roll. Its machine-direction tensile strength and ex-
tensional stiffness varied by a factor of 3 to 2 across the width of the roll.
This was, undoubtedly, an edge roll off the paper machine, but even so, the

variability was surprisingly large. The variability in properties is shown in
Table XIX of the appendix. It is graphically illustrated by the set of M.D.
stress-strain curves obtained on the Instron tester on 1-inch-wide strips taken
across the width of the roll (see Fig. 12). Note that despite the wide differences
in strength, the stretch (extension at rupture) is about the same across the
roll. The stress-strain curve of full width specimens is approximately that
of Position 7.

The results of the large-specimen tensile fracture tests on the bag
paper are summarized in Table XIV. They show, as might be expected, that cuts
of similar length produce different results if placed in the weak versus the
strong edge of the specimens. Cuts placed in the weak edge result in higher
critical stresses. These critical stresses are not characteristic of the material
at the crack tip. The properties of paper distant from the cut have little
influence on whether fracture occurs, but continue to influence the total load
borne by the specimen. For example, a cut of 100-mm length in the strong side
leaves largely low modulus material in the residual or net section. This should
result in lower critical stresses, which are, in fact, observed. Conversely,
cutting into the weak edge an appreciable distance leaves the high-modulus
material in the net section and consequently results in higher critical stresses
than normal. Critical stress versus cut length data become quite distorted with
such extreme variability in M.D. properties across the width of the specimen.

It was noted that when no cuts were made specimen failure originated
at the weak edge. When cuts of 3.18-mm length were introduced into the weak
edge, they did not always result in failure at the cut. When a 3.18-mm cut was
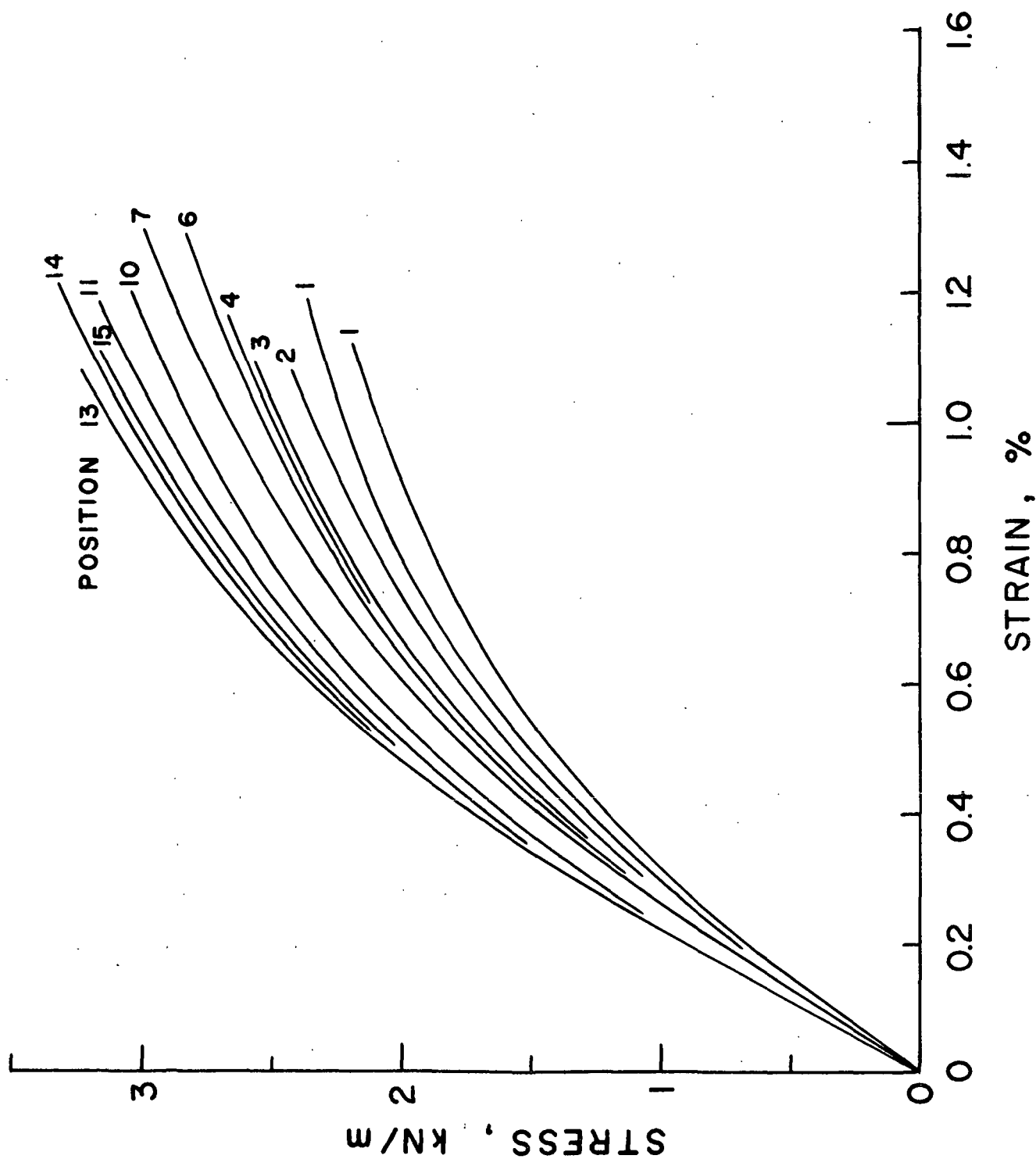placed in the strong edge, it always produced failure at that site.

Figure 12. Stress-Strain Curves for 1-inch-Wide Specimens of Bag Paper Taken Across the Width of the Supply Roll. 50% RH

TABLE XIV

LARGE-SPECIMEN FRACTURE PROPERTIES OF BAG PAPER AT 50% RH

Number of Tests	Initial Cut Length, a, mm	Critical Stress, $\sigma_c t$, N/m	Critical Strain, ε_c, %	Extensional Stiffness, Et, kN/m	$\sigma_c t \sqrt{a}$, N·m$^{-1/2}$	$\varepsilon_c \sqrt{a}$, m$^{-1/2}$ x10^4	$\dfrac{(\sigma_c t)^2 \sqrt{a}}{Et}$, N·m$^{-1/2}$	Net Section Stress, σ_N, N/m
6	0	2590	0.94	—	—	—	—	2590
4	W-6.35[a]	1740	0.48	410	139	3.82	0.59	1769
4	W-12.7	1410	0.37	405	159	4.17	0.55	1459
3	W-25.4	1117	0.30	385	178	4.78	0.52	1197
4	W-50.8	1070	0.29	380	241	6.53	0.68	1235
4	W-101.6	885	0.26	345	282	8.29	0.72	1207
3	S-3.18	2270	0.71	415	128	4.00	0.70	2289
4	S-6.35	1590	0.44	405	127	3.51	0.50	1617
4	S-12.7	1120	0.29	405	126	3.27	0.35	1159
4	S-25.4	1025	0.27	410	163	4.30	0.41	1098
4	S-50.8	915	0.25	380	206	5.63	0.50	1056
4	S-101.6	695	0.23	320	222	7.33	0.48	948

[a]The W and S prefixes indicate placement of the cut in the weak and strong edges, respectively.

We wish, of course, to estimate the load-carrying capacity of strong and weak bag paper in the large- and small-cut-length regimes, respectively, using data obtained on specimens of varying quality. A first approach to estimate the proper critical stresses for the weak and strong side material is to assume that the critical strain values do properly represent the material quality. This assumption would be supported, for example, if the critical strain were no different when a specimen of half-width was tested. Unfortunately, the lower critical strain values were not obtained very accurately in these Baldwin tests. Proceeding further, it will next be assumed that the stress-strain curve at Position 3 (Fig. 12) properly describes the response of material on the weak side when a 50.8-mm cut is present and that the curve at Position 13 applies to the same cut length on the strong side. Taking the critical strain values from Table XIV, a critical stress at this cut length of about 1190 N/m was estimated for strong-side substance and about 1050 N/m for weak-side substance. These are both high estimates since the apparent elastic modulus of specimens having this cut length is only about 93% of the modulus of an uncut specimen. Using the same critical strains, and estimates of the apparent Young's modulus of cut specimens, the estimated strong-side and weak-side critical stresses at 48-mm cut length are 1060 and 960 N/m, respectively. This estimating technique does predict greater critical stresses for specimens comprised wholly of strong-edge material than for specimens comprised wholly of weak-edge material.

One can now examine this bag paper sample with respect to the correlation of Fig. 9 in which the critical stress at 48.3-mm cut length was related to the square root of the product of the C.D. in-plane tearing strength and the M.D. extensional stiffness. The data involved in making an estimate of the critical stresses using the relationship of Fig. 9 are given below. These

data were derived from the physical property profiles given in Table XIX of the appendix.

	Weak-Edge Material	Strong-Edge Material
C.D. in-plane tearing strength, g-cm/cm	100	110
N-m/m	0.98	1.08
M.D. extensional stiffness, kN/m	355	455
$(U_{cd} \times Et_{md})^{1/2}$	590	700
$(\sigma_c t)_{48.3}$ (estimated using Fig. 9), N/m	910	1150
$(\sigma_c t)_{48.3}$ (calculated from ε_c and Et), N/m	960	1060

Considering all of the error inherent in the above procedure, the agreement in the critical stress estimates is quite good. It appears that the simple correlation of Fig. 9 is useful in predicting the critical stress level of commercial papers in the large-cut-length regime.

The critical stress for the strong-edge material at a cut length of 3.33 mm was estimated from the critical strain and stress-strain curve at Position 13 at about 2600 N/m. The correlation of Fig. 10, an extensional stiffness of 455 kN/m, and a C.D. in-plane tear strength of 1.08 N, yields an estimated critical stress of 2500 N/m. This, too, represents excellent agreement and demonstrates the value of the correlation of Fig. 10 for the prediction of the load-carrying capacity of large webs at small cut lengths. This correlation also needs to be tested with a still broader array of samples. On the basis of the results already obtained, however, it is recommended for use until a better means of dealing with paper fracture quality is developed.

THE EFFECT OF SPECIMEN SIZE AND SHAPE

Some understanding of the effects of specimen size and shape on the tensile fracture behavior of paper containing cracks is needed to improve our understanding of fracture behavior generally, to permit the extension of the experimental results to webs of still larger size, and to develop efficient testing methods to obtain the needed information using small specimens. There may be little need for wider specimens when working within the small-edge-cut-length regime. Length to width ratio may be another matter, however.

Length to width ratios of 3:1 or greater are considered desirable in tensile fracture studies to minimize length/width ratio effects on the results. In the Baldwin tests, a ratio of 3.33 to 1 was used. This increased to 5.25 to 1 in the tests on the LSTT instrument. Bowie and Neal (11) computed, for linear elastic isotropic specimens containing a single edge crack equal to 10% of the specimen width, that the stress intensity factor at $L/w = 1$ is only about 3% greater than that at $L/w = 3$. This would increase to 8.7% with an edge crack equal to 30% of the specimen width.

Walsh (12) analyzed the specimen length/width ratio effect for the case of highly oriented, planar, orthotropic materials. He noted that an L/w ratio of about 6 is needed in very highly oriented materials before the stress intensity factor (from LEFM theory) remains essentially constant with increasing ratio. At a L/w ratio of 1.5, the stress intensity factor was only about 10% greater than that computed for a specimen of infinite length, but as the length/width ratio became still smaller, the stress intensity factor rose sharply. At $L/w = 1.2$, the stress intensity factor was about 30% greater than that of the infinite length specimen. Although commercial paper samples are not nearly as oriented as the

example chosen for analysis by Walsh, it is also clear that the L/w ratio effects
expected for isotropic elastic materials will not be applicable.

In a few tests performed on web-offset paper on the Baldwin tester,
the following results were obtained. For specimens of 190.5-mm width and
1270-mm length (L/w = 6.67), the average critical stress was reduced by about
5% from that obtained at 381-mm width and 1270-mm length (L/w = 3.33). When
the specimen length was reduced to 635 mm at the 381-mm width (L/w = 1.67), the
critical stress increased by about 11% over that obtained at the L/w ratio of
3.33. This result was of interest and tests at various L/w ratios were under-
taken later with the bag paper. This proved to be an unfortunate choice of
sample in view of its nonuniform quality, but the results do show the kinds of
effects which might be expected generally.

In examining the effect of L/w ratio on the strength of kraft bag paper
specimens, width was held constant at 381 mm and test lengths of 102, 254, 635,
and 1270 mm were used. Tests were run both without cuts and with single edge
cuts of 6.35, 12.7, and 50.8 mm. A few tests were also made employing cuts at
both edges and with cuts introduced at the center of the specimen. All cuts were
perpendicular to the length direction and mid-distant between the clamps. The
results are presented in Table XV. As seen before with this sample, the critical
stresses varied with the edge in which the cut was made.

It should be noted that in most of these tests fracture occurred at
critical stresses and strains exceeding the limit of Hookian response. Apparent
elastic response to the point of fracture was noted only for the longest specimens
(1270 mm) with the largest initial edge cut (50.8 mm).

TABLE XV

EFFECT OF SPECIMEN LENGTH ON TENSILE PROPERTIES OF KRAFT BAG PAPER[a]

Specimen Length, mm

Initial Cut Length, mm	Cut Location	102[b]		254			635			1270		
		No.[c]	$\sigma_c t$[d]	No.	$\sigma_c t$	ε_c[e]	No.	$\sigma_c t$	ε_c	No.	$\sigma_c t$	ε_c
0	--	5	3040	5	2850	1.03	5	2690	0.98	6	2590	0.91
6.35	Edge 1	--	--	3	2610	0.93	--	--	--	4	1740	0.48
12.7	Edge 1	3	2940	3	2550	0.91	3	1870	0.54	4	1410	0.37
50.8	Edge 1	1	2490	3	1870	0.63	--	--	--	6	1060	0.30
6.35	Edge 2	--	--	3	2170	0.67	--	--	--	4	1590	0.44
12.7	Edge 2	3	2750	3	2260	0.77	3	1600	0.41	4	1120	0.29
50.8	Edge 2	1	2370	3	1690	0.60	--	--	--	2	785	0.22
12.7	Center	1	2510	--	--		--	--		--	--	--
50.8	Center	1	1820	--	--		--	--		--	--	--
12.7	1 & 2	--	--	--	--		--	--		1	1140	0.31
50.8	1 & 2	--	--	--	--		--	--		1	765	0.24

[a] All tests at 50% RH, 23°C; rate of straining = 6%/min.

[b] Critical strains could not be determined accurately at this test span.

[c] Number of tests.

[d] $\sigma_c t$ = Critical stress, N/m.

[e] ε_c = Critical strain, %.

The results plotted in Fig. 13 are for cuts in the weak edge (Edge
1) only. They illustrate that the greatest effect of an edge flaw occurs in
specimens of greatest length. When the specimen length was reduced to very
small values, small edge cuts had very little effect on sheet tensile strength.
For example, an initial edge cut of 12.7 mm in the weak edge of a bag paper
specimen 102-mm long ($\underline{L}/\underline{w}$ = 0.267) resulted in a critical stress reduction of
only about 3.3%, which is equal to the reduction in net section width. At the
same specimen length, a 50.8-mm edge cut caused a strength loss only 5.5% below
that of an uncut specimen when compared on net remaining or uncut width basis.
The fractures appeared to be unstable in all of these tests. It is always
possible, of course, that some stable fracture occurred prior to the onset of
sudden unstable fracture, but if so, it occurred only to a very slight extent
and was neither observed directly nor indicated on the Baldwin tester load-
elongation plot.

In single tests at 1270-mm length and 381-mm width with double-edge
cuts of 12.7 and 50.8-mm length, the critical stresses were <u>very close</u> to those
obtained with single-edge cuts placed in Edge 2. This is expected for small
cut lengths. At the 50.8-mm cut length, one might expect critical stresses
for double-edge cuts to be about 10% higher than those obtained in single-edge
cuts if the correction factors of LEFM theory were applicable.

When a 12.7-mm cut was placed in the center of a specimen of 102-mm
test length, the critical stress was <u>lower</u> than that obtained with a single
edge cut of the same length. This is a rather surprising result, which
occurred also with a center cut of 50.8 mm at this test span. A center cut
of 12.7-mm length in the 1270-mm specimen resulted in failure at a critical
stress <u>well above</u> that obtained with an edge cut of that length and also
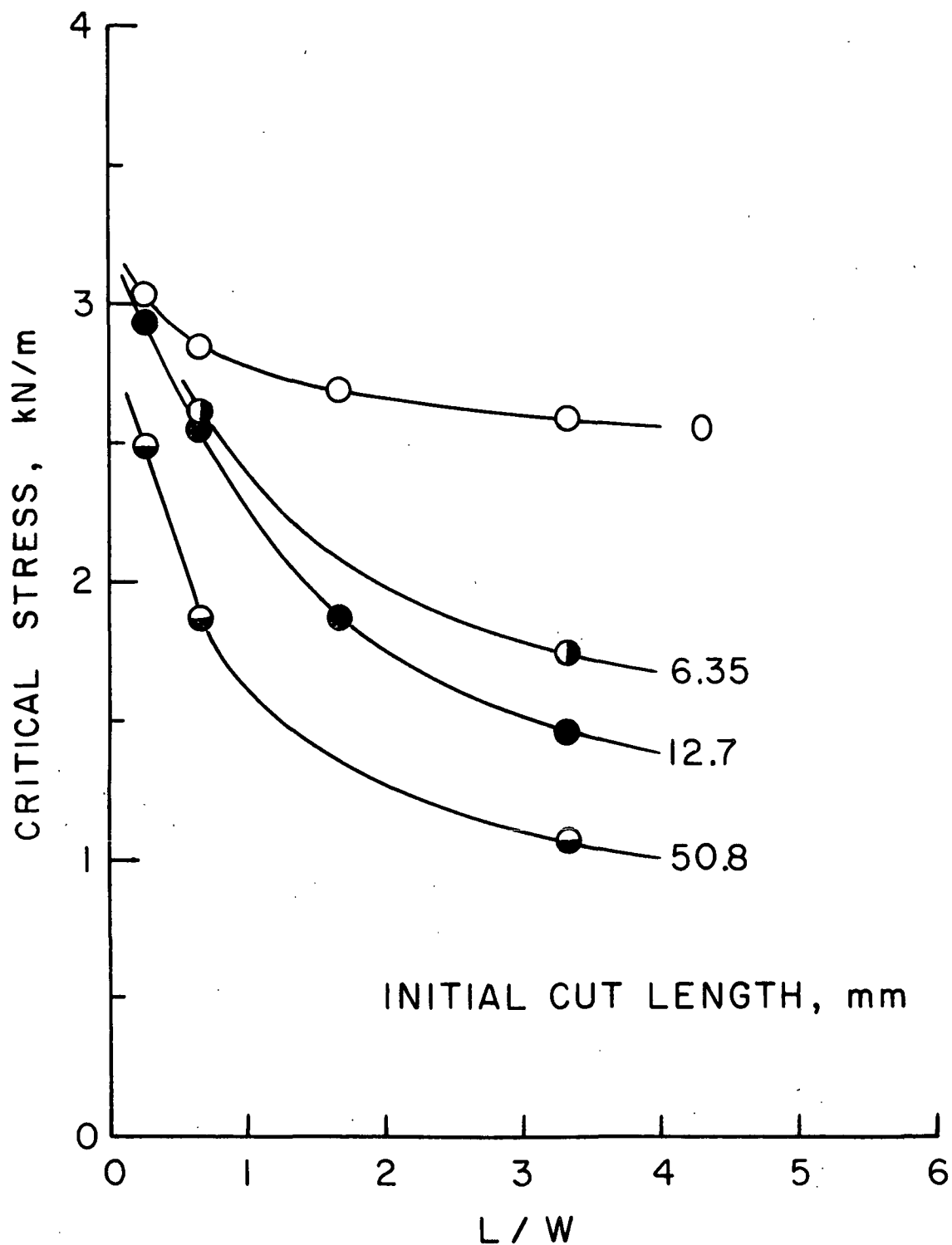
Figure 13. Effect of Length-to-Width Ratio on Critical Stress of Bag Paper
at Various Initial Single-Edge-Cut Lengths. Specimen Width
(w) = 381 mm

exceeded that obtained with 6.35-mm cuts in either Edge 1 or Edge 2. In LEFM

theory, a center cut must be twice as long as an edge cut to produce failure at

the same tensile load. For long specimens, the expected reduced sensitivity

to small flaws in the center of the specimen is supported by this single test

result even though the critical stresses well exceed the elastic limit. On

the other hand, the unexpected, rather pronounced strength reducing effect of

center cuts in specimens of very low L/w ratio deserves additional attention.

Some applications of paper may involve such dimensions and specimen restraints.

The effect of flaw dimensions on the service strength of paper subjected to

biaxial loads may be particularly relevant to these observations about center

cracks in specimens of low L/w ratio.

These few data do not by any means clarify the matter of specimen

dimensions on fracture behavior. For example, how is one to consider a web

of 120-inch width with an open draw of 60 inches? Is the data acquired at an

L/w ratio of 0.5 applicable if obtained using a 15-inch specimen width?

CRACK PROPAGATION VELOCITY.

The rate of crack propagation in unstable fracture is a subject of

considerable interest in fracture mechanics. Crack velocities depend on

material properties, and, in theory, on the energy release rate at any time

relative to the fracture resistance of the specimen. Hence, they depend on

the specimen dimensions, initial and extended crack dimensions, rate of loading,

etc. Crack velocity is of major interest where materials or structures can

be modified to stop the growth of a crack after it has progressed unstably for

some distance; i.e., crack arrest. Though crack arrest, apparently, is not

common in paper web transport situations, it may be of interest in other applications of paper.

Some exploratory work was undertaken to measure crack propagation velocities in large-specimen tensile tests of web-offset paper at several initial cut lengths. An experimental technique was used which involves placement of an electrically-conductive resistor grid onto the specimen surface in the expected path of the fracture. The grid was drawn on the specimen surface with a dispersion of graphite in a nonaqueous medium. It consisted, as shown in Fig. 14, of a number of parallel resistors oriented perpendicularly to the line of expected fracture. A "trigger" resistor was placed between the tip of the crack and the grid. When the unstable fracture advanced to break the trigger resistor, an oscilloscope sweep circuit was activated at an appropriate rate. The resistor grid controlled the voltage applied to the vertical input of the oscilloscope. As the crack progressed to break the first parallel resistor of the grid, the resulting change in voltage was readily indicated on the oscilloscope display. Successive ruptures of the grid resistors were also indicated in this manner. Knowing the sweep rate and the distance between the voltage steps on the oscilloscope display, the elapsed time between fractures of the grid resistors was determined. Since the dimensions of the resistor grid are known, an average velocity of crack propagation can be calculated for each of the various distance intervals. This technique is subject to a number of errors which are most serious in the period of increasing crack velocity but of little importance when the crack velocity becomes relatively constant.

Attempts were made to acquire data without edge cuts and with initial cuts 3.18, 12.7, and 50.8 mm in length. Without initial cuts, the fractures began near the clamp and progressed obliquely across the specimen. Uncertainty
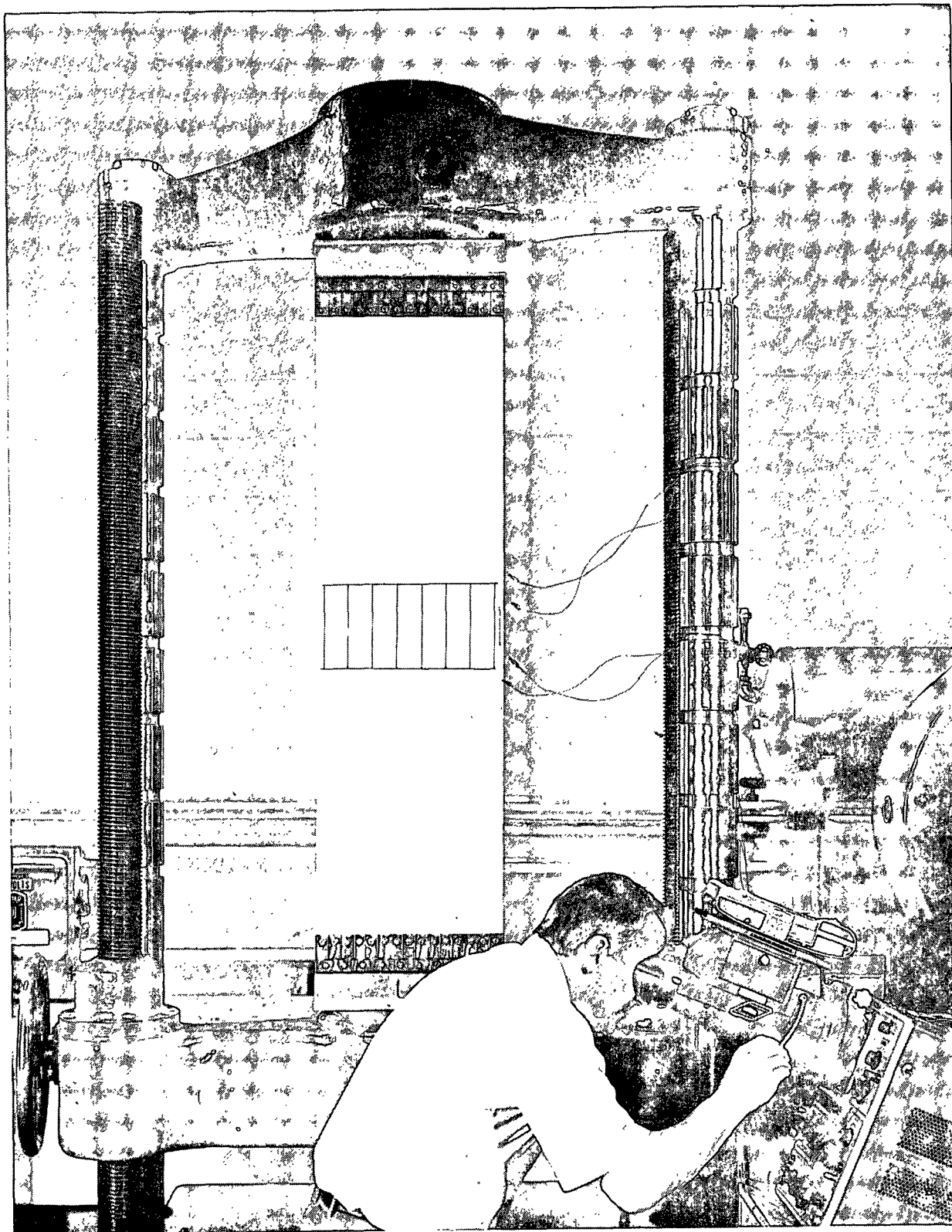
Figure 14.   Large Specimen with Electrical Resistor Grid in Baldwin Tester
Prior to a Crack Velocity Determination

about the position of the fracture line and the very low incidence of fracture

across the central region of the specimens discouraged attempts to obtain such

data on uncut specimens. Good results were obtained, however, for specimens

containing 3.18 and 12.7-mm single-edge cuts. The crack velocities are plotted

versus distance for these two cases in Fig. 15. The horizontal lines drawn

on the graph indicate the average crack velocities and the positions on the

specimens where these averages apply. The results of tests on three different

specimens are presented in each figure.

In tests performed with 12.7-mm edge cuts, the initial crack velocity

was low. For example, in one such test, an average velocity of only 0.8 m/s

was determined for the interval 9 to 19 mm from the cut tip. Over the interval

20 to 80 mm from the cut tip, the crack velocity was still only about 50 to

60 m/s. Though these velocities are low relative to the maximum velocities

recorded in these tests, they are much too high to be assessed by the unaided

eye. For example, at 50 m/s, a crack would progress a distance of 5 cm in one

millisecond. At the 12.7-mm cut length, the crack velocity increased rather

sharply in the distance interval of about 80 to 120 mm from the tip of the initi-

ating cut and reached velocities exceeding 700 m/s. At velocities of this

magnitude, achieved in this case when the crack was 200 to 250 mm in length,

"crack branching" was observed. Crack branching is the development of multiple

running cracks (usually only two at a time) which may progress simultaneously

for some distance. The branch crack may stop after travelling a short distance,

new branch cracks may then develop, etc. It was noted that usually (but not

always), when crack branching occurred in any distance interval, the crack

velocity dropped within that interval to lower values. This, undoubtedly, is due

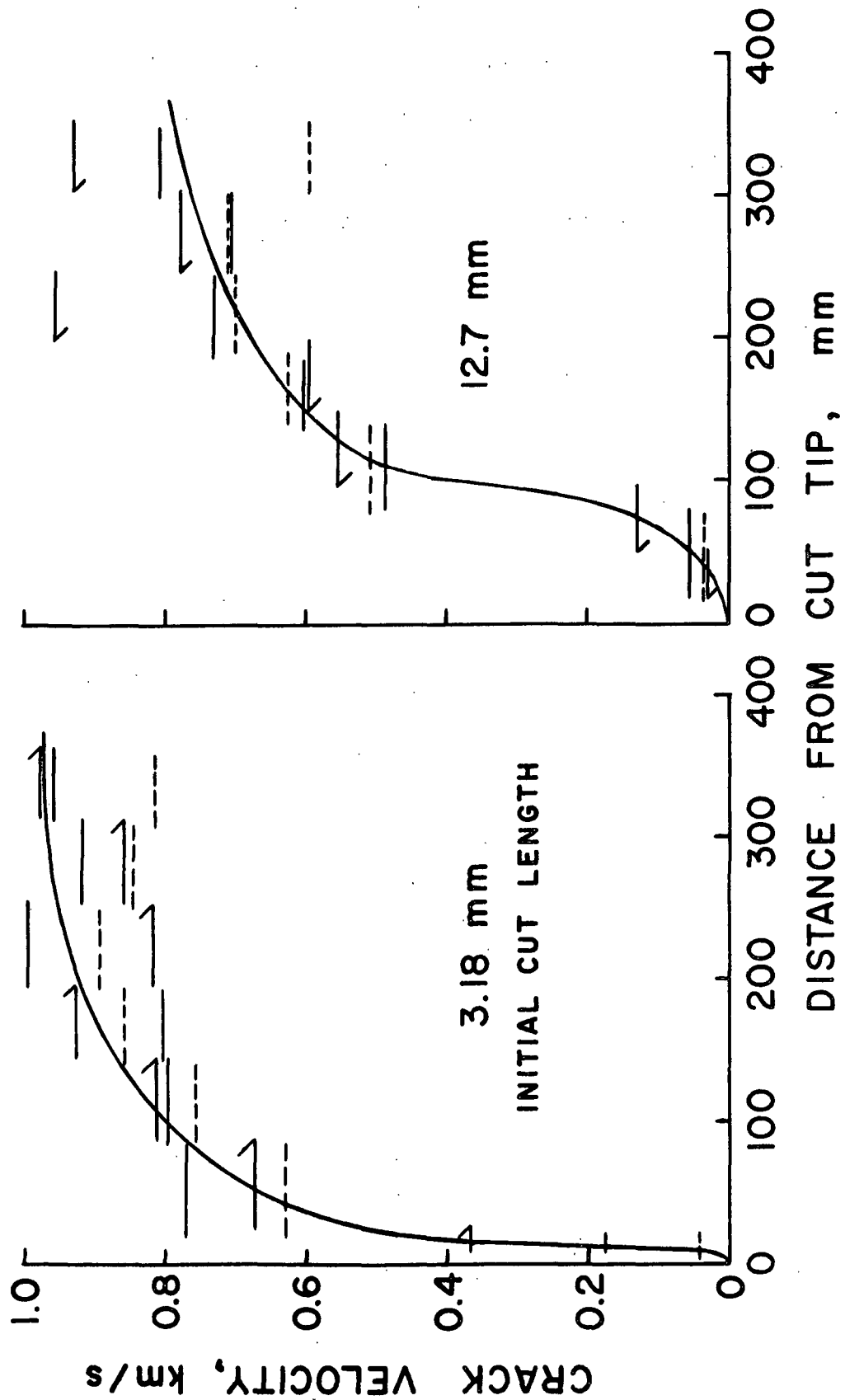to the increased dissipation of energy with branching. Crack branching was not

Figure 15. Average Crack Velocities Versus Distance from Cut Tip in Tests of Offset Paper with Single Edge Cuts of 3.18 and 12.7 mm. 50% RH

evident at velocities below about 700 m/s and was never noted at very low velocities. Crack branching is illustrated in Fig. 16 for a specimen of web-offset paper tested at an initial cut length of 3.18 mm. One may observe in this photograph the more orderly progression and appearance of the fracture line when the crack velocity was low initially (near the bottom of Fig. 16) and the ragged fracture occurring later at high velocities. Note also that in this specimen the last branched crack and the main crack proceeded together over a distance of about 65 mm to complete fracture of this specimen.

The development of branching in running cracks is a phenomenon associated with brittle materials. It apparently does not occur in materials exhibiting appreciable plastic flow. Thus, in this respect, paper is a brittle material. The preferred means of characterizing crack branching behavior is through a crack branching stress intensity factor, employing for this purpose the length of the running crack at which crack branching just begins. Congleton (13) views crack branching as the result of the development of advance cracks ahead of the main running crack, which, having attained adequate size, velocity, and direction, can proceed without being absorbed by the main running crack. Where LEFM theory applies, the stress intensity factor for crack branching is reported to be about 1.4 times the normal stress intensity factor for very brittle materials such as glass and up to 4 times greater for various metals and glassy polymers. It is difficult to determine the onset of crack branching in paper and to establish a critical stress intensity factor for the onset of branching. It would appear, however, that a value four times greater than that at the onset of unstable fracture is of proper order of magnitude.

In tests at 3.18-mm initial cut length, the crack velocity accelerated to high values very close to the cut tip. The crack velocity was low for a
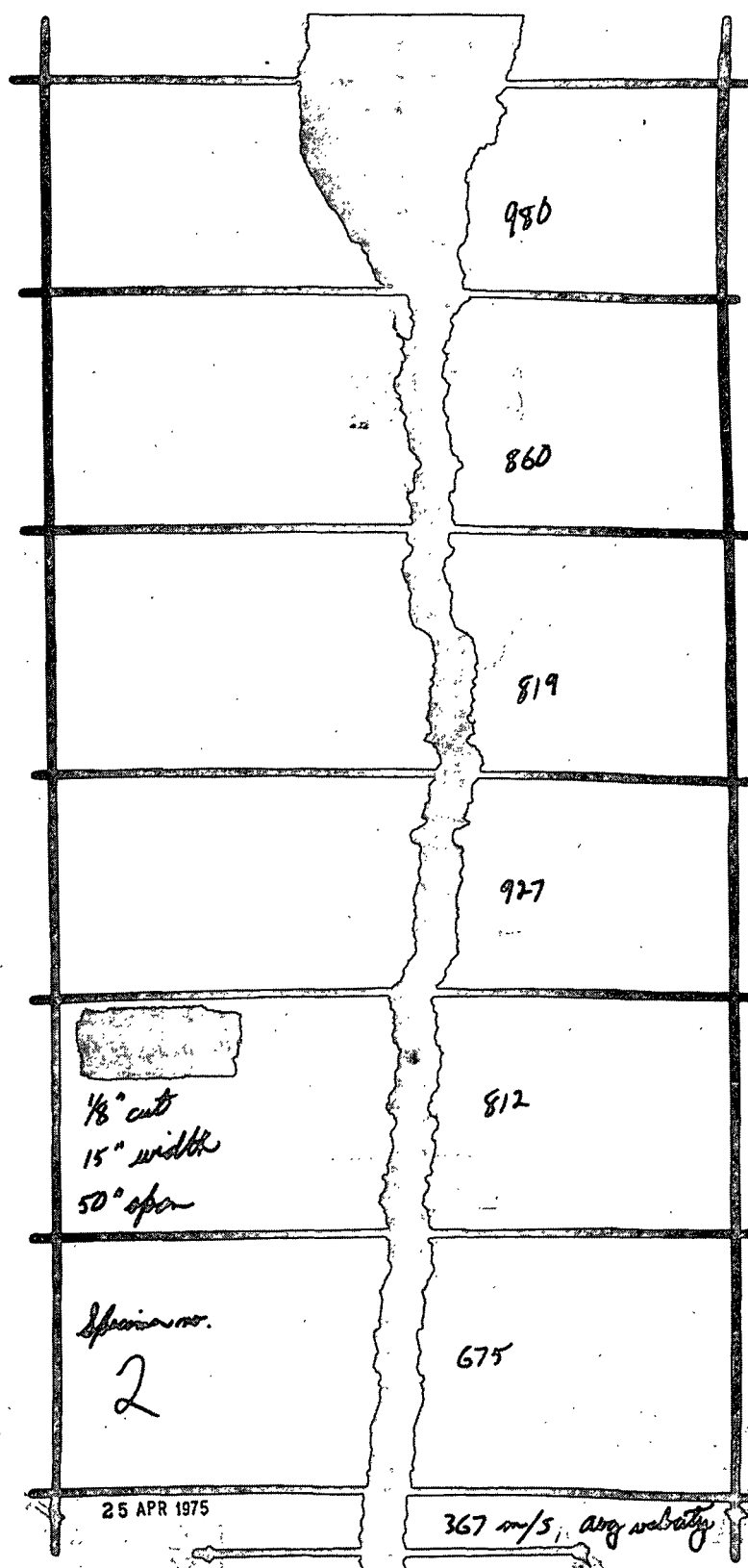
Figure 16.   Fracture Zone of Web-Offset Paper After Test at Initial Cut
Length 3.18 mm; 50% RH. Note Crack Branching

rather short distance prior to rapid acceleration. Better data could, of course, be obtained in this region if desired.

In tests at initial cut lengths of 50.8 mm, the crack velocity proved to be much too low over the entire remaining width of the specimen for accurate measurement using this oscilloscope technique. For three of the tests attempted at this cut length, the crack velocity could be estimated only within the last interval of the resistor grid. The three crack velocities for this last interval were 1, 2.5, and 4 m/s. Such very low values so near to completion of fracture of the specimen indicate no tendency for acceleration within the 381-mm width of these specimens and also suggest that the energy release rate is more nearly in balance with the fracture resistance of this paper in these larger initial-cut-length tests.

Maximum crack velocities of about 1000 m/s were recorded in these tests on web-offset paper. This exceeds values of 500 to 900 m/s reported by Glover, Johnson, and Radon (14) for polycarbonate, polyvinyl chloride, polystyrene, and nylon in bending-type fracture tests at room temperature, but falls within the range of maximum velocities of 700 to 2150 m/s reported for various types of glass (15). From the various theoretical and experimental values reported in the literature, one may expect maximum crack velocities (before branching occurs) in the range of 0.2 to 0.4 of the longitudinal wave velocity of the specimen. Thus, since the longitudinal wave velocities of paper easily attain values of 2000 to 5000 m/s, the 1000 m/s values determined in these tests are typical of other materials in this respect. The longitudinal wave velocity was not measured for the web-offset paper.

The Fracture Zone

Virtually nothing is yet known about the stress and strain distributions surrounding the tip of a crack in paper under tensile load. One readily observes, of course, that prior to unstable fracture there exists a zone immediately surrounding the tip of an initially sharp cut in which debonding of the fiber network structure occurs. In large-specimen tests, this zone extends only very short distances beyond the tip of the cut, usually of the order of the average fiber length or less. There is presently no information available which would indicate the magnitudes of stress or strain in the more or less intact structure immediately adjacent to this zone of network disintegration. From observations of the condition of the fracture surfaces during the relatively slow period of crack growth at the beginning of the unstable fracture process and those noted at high crack velocities, it seems reasonable to assume that the stress and strain fields at the tip of the crack before unstable fracture differ from those surrounding the rapidly running crack. Nonetheless, it was felt that some further insight might be gained by high-speed photographic recording of the state of the running crack. Such photographs are shown in Fig. 17 for cracks of various stages of progression, all initiated from an initial cut of 3.18-mm length in specimens 381 mm wide. In the first photograph, at the upper left, the crack progressed a distance of only about 30 mm. The crack had not yet opened to any significant extent. In the photograph at left center, the crack length is about 135 mm and there is still very little opening of the crack. This is, of course, not surprising, since at a critical strain of about 0.6%, the total possible elastic recovery of the specimen is only about 5 mm.
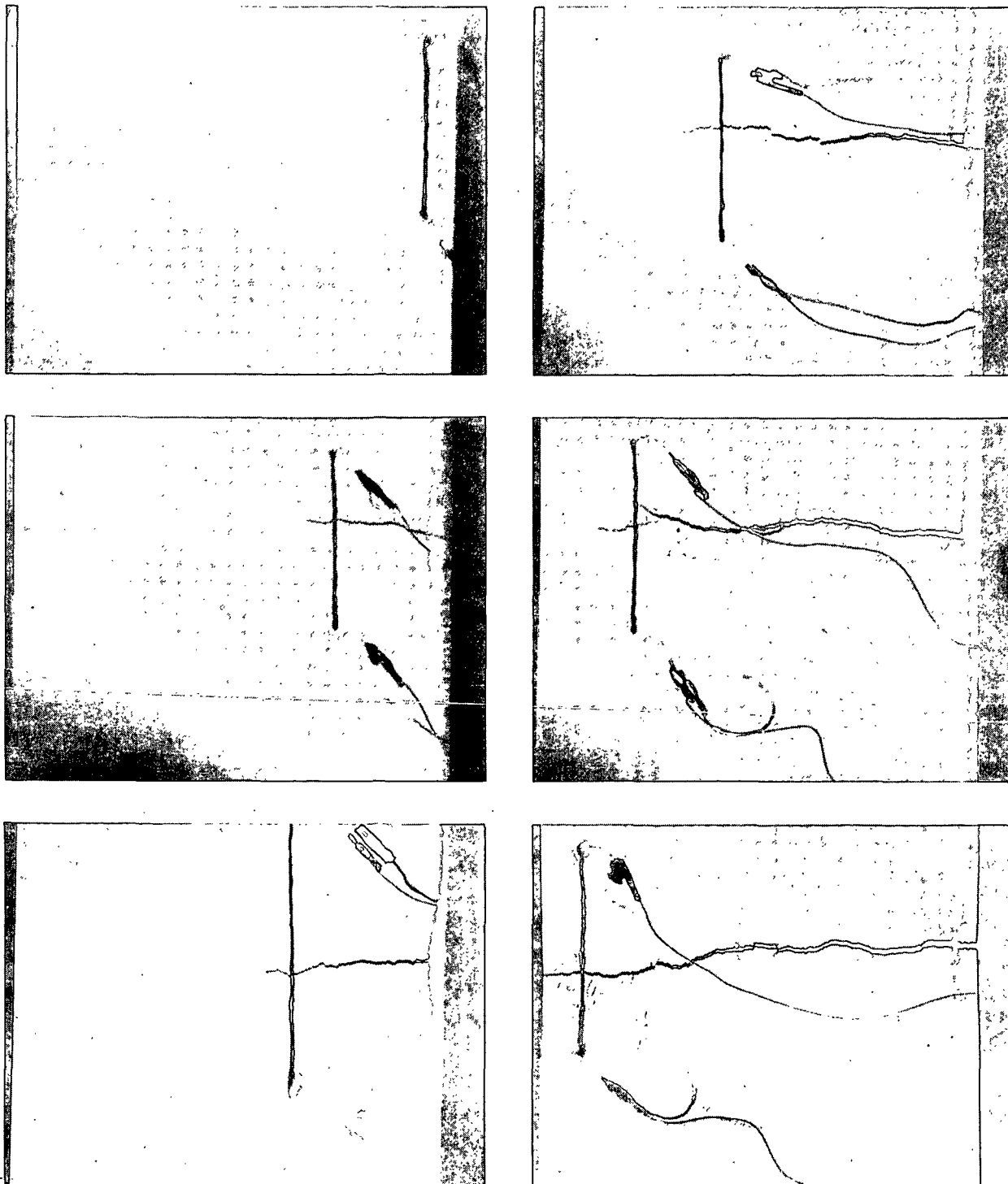
Figure 17. Microflash Photographs of Running Cracks in Large Specimens of
Web-Offset Paper. Each Photograph is of a Different Specimen

For the same conditions of testing, photographs were obtained in the vicinity of the "tip" of the running crack. These are shown in Fig. 18 using reflected and transmitted light. The vertical reference lines are 25.4 mm apart. There is no readily detectable "crack tip" in these photographs. Rather, one is inclined to view the tip of a rapidly advancing crack as a blurred zone of appreciable length in the direction of the propagating crack in which stresses probably exist of a magnitude sufficient to cause disintegration of the structure. On the other hand, the structural disintegration is confined to a rather narrow zone perpendicular to the crack.
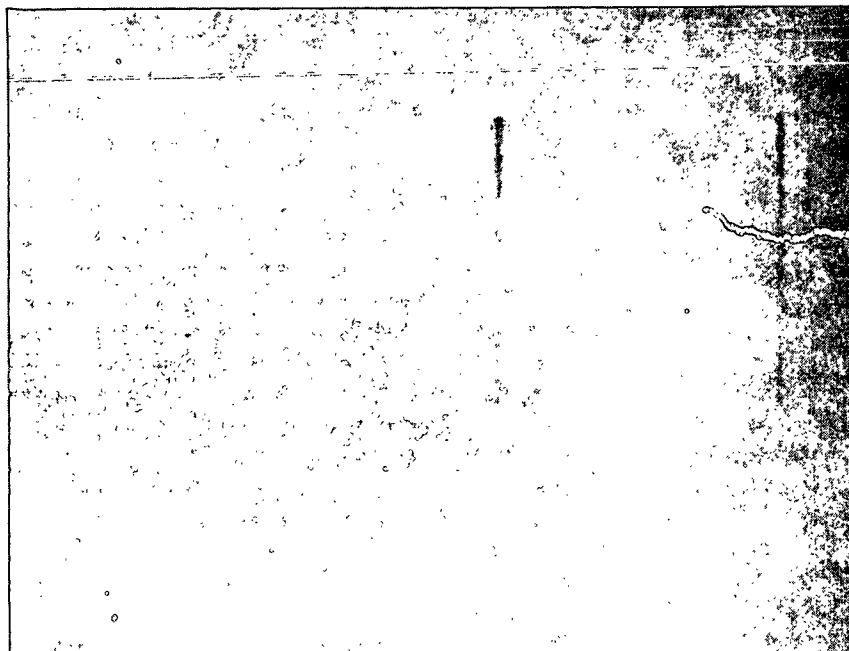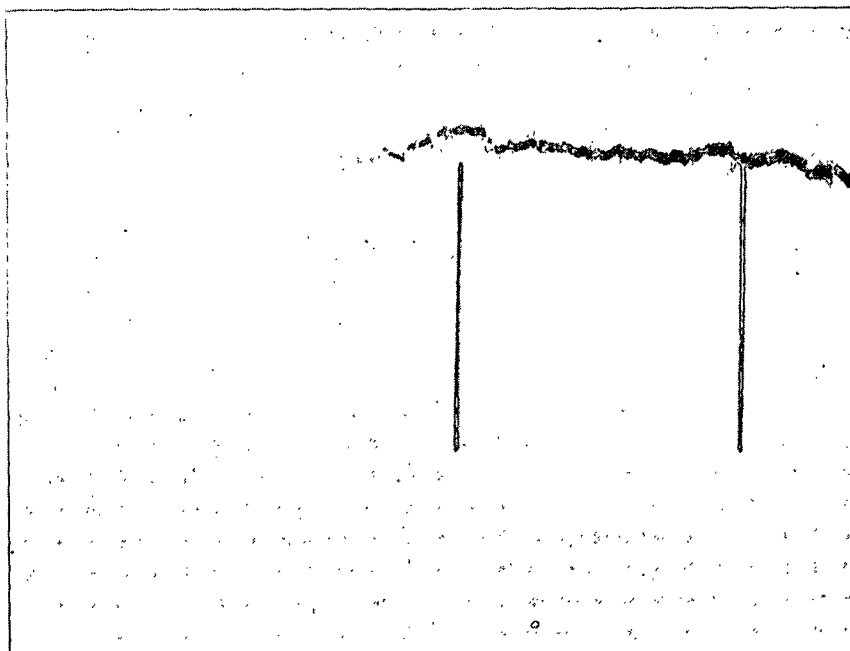
Figure 18.   Enlarged Zone of Running Crack in Web-Offset Paper Viewed
by Reflected and Transmitted Microflash Illumination
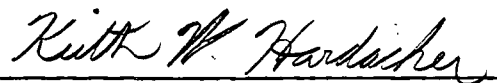
NOMENCLATURE

$\underline{a}$ characteristic crack length dimension, length of initial cut in edge of specimen

$\underline{a}^*$ corrected crack length

$\underline{b}$ characteristic specimen width dimension

$\underline{E}$ Young's modulus

$\underline{Et}$ extensional stiffness, product of Young's modulus and thickness

$\underline{Et}_{\underline{md}}$ extensional stiffness in the machine direction

$\underline{F}(\underline{a}/\underline{b})$ finite specimen-size correction factor

$\underline{G}$ energy release rate (also fracture energy, crack extension force)

$\underline{K}_{\underline{c}}$ critical stress intensity factor

$\underline{L}$ specimen length

$\underline{t}$ thickness of paper specimen

$\underline{U}_{\underline{cd}}$ in-plane tearing strength in the cross-machine direction

$\underline{w}$ specimen width

$\varepsilon_{\underline{c}}$ critical strain (average strain of entire specimen at moment of unstable fracture)

$\sigma_{\underline{c}}$ critical stress based on total cross section of specimen ignoring the edge cut

$\sigma_{\underline{c}}\underline{t}$ the product of critical stress and sheet thickness

$\sigma_{\underline{n}}\underline{t}$ critical stress computed on net uncut section
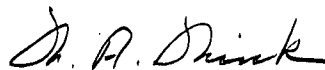
LITERATURE CITED

1. Sears, G. R., Tyler, R. F., and Denzer, C. W., Pulp Paper Mag. Can. 66 (7):T351-60(July, 1965).

2. Balodis, V., Australian J. Appl. Sci. 14:284-304(1963).

3. Anderson, O., and Falk, O., Svensk Papperstid. 69(4):91-9(Feb. 28, 1966).

4. Seth, R. S., and Page, D. H., J. Materials Sci. 9(11):1745-53(1974).

5. Seth, R. S., and Page, D. H., Tappi 58(9):112-17(Sept., 1975).

6. Fracture toughness testing and its applications. STP 381 (ASTM, Philadelphia, 1965), 409 p.

7. Broek, D. Elementary engineering fracture mechanics. Leyden, Noordhoff International Publishing, 1974. 408 p.

8. Knauss, W. G., Appl. Mech. Rev. 26(1):1-17(Jan., 1973).

9. Paris, P. C., and Sih, G. C. In Fracture toughness testing and its applications. p. 40-4. STP 381 (ASTM, Philadelphia, 1965).

10. Fracture testing of high strength sheet materials. First Report of Special ASTM Committee, ASTM Bulletin, Jan., 1960.

11. Bowie, O. L., and Neal, D. M. Trans. ASME 32E (J. Appl. Mech.) 3:708-9 (Brief Notes) (Sept., 1965).

12. Walsh, P. F., Eng. Fracture Mechanics 4:533-41(1972).

13. Congleton, J. In Sih's Dynamic crack propagation. p. 427-38. Leyden, Noordhoff International Publishing, 1973.

14. Glover, A. P., Johnson, F. A., and Radon, J. C., In Sih's Dynamic crack propagation. p. 227-59. Leyden, Noordhoff International Publishing, 1973.

15. Kerkhof, F. In Sih's Dynamic crack propagation. p. 3-35. Leyden, Noordhoff International Publishing, 1973.
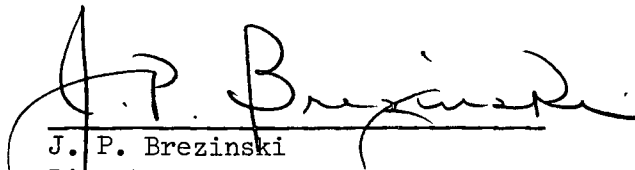
THE INSTITUTE OF PAPER CHEMISTRY

Keith W. Hardacker
Research Fellow
Division of Materials
Engineering & Processes

W. A. Wink
Research Associate
Division of Materials
Engineering & Processes

J. P. Brezinski
Director
Division of Materials
Engineering & Processes

APPENDIX

TABLE XVI

PROFILE OF PHYSICAL PROPERTIES ACROSS WEB FOR WEB-OFFSET PAPER AT 50% RH

Position in web

		1	2	3	4	5	6	7	9	10	11	12	13	14	15
Basis weight, g/m²		48.1	47.7	48.3	48.0	48.0	47.8	47.7	47.7	47.7	47.6	47.2	47.5	47.7	48.1
Thickness, µm		61.0	60.5	61.5	60.5	61.0	61.0	58.9	59.4	60.5	59.4	59.4	58.4	58.4	59.4
Tensile strength, N/m	MD	2840	2900	2970	2890	2940	2960	2940	2880	2960	2820	3000	2970	2970	2970
	CD	1590	--	--	--	--	--	--	--	--	--	--	--	--	1520
Stretch, %	MD	1.52	1.54	1.57	1.51	1.51	1.02	1.45	1.41	1.48	1.36	1.62	1.57	1.58	1.53
	CD	4.04	--	--	--	--	--	--	--	--	--	--	--	--	3.63
TEA, kg-m/m²	MD	2.87	2.94	3.07	2.91	2.93	2.99	2.81	2.58	2.88	2.53	3.22	3.11	3.12	3.00
	CD	4.91	--	--	--	--	--	--	--	--	--	--	--	--	4.26
E_t, kN/m	MD	412	409	416	413	421	429	430	427	427	424	416	416	412	425
	CD	215	--	--	--	--	--	--	--	--	--	--	--	--	210
Zero-span tensile strength, kg/cm	MD	6.38	6.32	6.26	6.38	6.38	6.35	6.20	6.23	6.35	6.17	6.32	6.26	6.23	6.32
	CD	4.78	4.78	4.96	4.78	4.99	4.90	4.99	4.87	4.99	4.99	4.96	4.81	4.96	4.87
In-plane tear, g-cm/cm	MD	55.8	--	--	--	--	--	--	--	--	--	--	--	--	53.2
	CD	53.0	--	--	--	--	--	--	--	--	--	--	--	--	54.2
Elmendorf tear, g-cm/cm	MD	60.8	--	--	--	--	--	--	--	--	--	--	--	--	62.8
	CD	58.4	--	--	--	--	--	--	--	--	--	--	--	--	54.8

The test material was conditioned and tested at 50% RH, 23°C. The moisture content was within the range of 5.66 to 5.72%.
The stretch, TEA, and E_t results have been corrected for instrumental strain error.

TABLE XVII

PROFILE OF PHYSICAL PROPERTIES ACROSS WEB FOR BOND PAPER AT 50% RH

Position in web

		1	2	3	4	5	6	7	9	10	11	12	13	14	15
Basis weight, g/m²		74.4	74.6	73.8	74.2	74.0	74.5	74.5	74.0	73.9	73.7	74.0	73.7	73.5	73.2
Thickness, μm		101	101	100	100	101	101	102	100	101	100	100	102	101	101
Tensile strength, N/m	MD	3860	3820	3780	3785	3830	3910	3870	3780	3770	3740	3780	3790	3760	3750
	CD	2550	—	—	—	—	—	—	—	—	—	—	—	—	2490
Stretch, %	MD	1.44	1.40	1.42	1.39	1.46	1.47	1.43	1.37	1.38	1.41	1.45	1.40	1.38	1.47
	CD	2.78	—	—	—	—	—	—	—	—	—	—	—	—	2.62
TEA, kg-m/m²	MD	3.59	3.42	3.45	3.39	3.67	3.75	3.57	3.28	3.33	3.41	3.56	3.46	3.33	3.65
	CD	5.39	—	—	—	—	—	—	—	—	—	—	—	—	4.95
$\underline{Et}$, kN/m	MD	534	537	526	532	526	540	537	537	528	524	522	531	529	533
	CD	370	—	—	—	—	—	—	—	—	—	—	—	—	366
Zero-span tensile strength, kg/cm	MD	8.97	9.29	8.82	8.88	9.25	8.85	9.06	9.13	9.19	8.72	9.06	9.09	9.54	9.33
	CD	8.29	8.65	8.33	8.23	8.36	8.22	8.30	8.06	8.00	8.03	8.23	8.35	8.30	8.34
In-plane tear, g-cm/cm	MD	75.6	—	—	—	—	—	—	—	—	—	—	—	—	74.0
	CD	67.0	—	—	—	—	—	—	—	—	—	—	—	—	68.4
Elmendorf tear, g	MD	50.4	—	—	—	—	—	—	—	—	—	—	—	—	51.8
	CD	50.0	—	—	—	—	—	—	—	—	—	—	—	—	53.2

The test material was conditioned and tested at 50% RH, 23°C. The moisture content was about 5.9%. The stretch, TEA, and $\underline{Et}$ results have been corrected for instrumental strain error.

TABLE XVIII

PROFILE OF PHYSICAL PROPERTIES ACROSS WEB FOR KRAFT PAPER AT 50% RH

		1	2	3	4	5	6	7	9	10	11	12	13	14	15
									Position in web						
Basis weight, g/m²		83.6	83.2	82.8	82.5	82.6	82.4	82.7	82.5	82.1	81.5	82.7	81.9	82.1	82.5
Thickness, μm		81.3	79.8	80.3	81.3	79.8	78.7	79.2	82.8	79.8	79.8	79.8	82.8	80.3	80.3
Tensile strength, N/m	MD	9540	9750	10100	9600	9880	9840	9860	9880	9870	9810	10100	9480	9690	9460
	CD	4070	—	—	—	—	—	—	—	—	—	—	—	—	4100
Stretch, %	MD	2.21	2.27	2.40	2.25	2.31	2.31	2.32	2.31	2.35	2.38	2.43	2.24	2.33	2.24
	CD	4.37	—	—	—	—	—	—	—	—	—	—	—	—	4.45
TEA, kg-m/m²	MD	13.3	13.9	15.2	13.6	14.5	14.3	14.5	14.5	14.7	14.8	15.5	13.6	14.3	13.5
	CD	12.2	—	—	—	—	—	—	—	—	—	—	—	—	12.4
Et, kg/cm	MD	899	902	899	900	902	899	897	900	890	874	892	880	877	874
	CD	301	—	—	—	—	—	—	—	—	—	—	—	—	296
Zero-span tensile strength, kg/cm	MD	15.5	15.4	15.3	15.3	15.7	15.6	15.7	15.6	15.4	15.6	15.7	15.6	15.5	15.6
	CD	8.13	8.42	8.35	8.00	7.98	8.21	8.12	8.26	8.12	7.97	7.86	7.89	8.06	8.47
In-plane tear, g-cm/m	MD	67.2	—	—	—	—	—	—	—	—	—	—	—	—	67.8
	CD	96.4	—	—	—	—	—	—	—	—	—	—	—	—	95.0
Elmendorf tear, g	MD	42.8	—	—	—	—	—	—	—	—	—	—	—	—	43.8
	CD	54.8	—	—	—	—	—	—	—	—	—	—	—	—	58.4

The test material was preconditioned at 86% RH, 23°C; then conditioned and tested at 50% RH, 23°C. The moisture content was within the range of 7.72 to 7.75%. The stretch, TEA, and Et results have been corrected for instrumental strain error.

TABLE XIX

PROFILE OF PHYSICAL PROPERTIES ACROSS WEB OF BAG PAPER AT 50% RH

		1	2	3	4	5	6	7	8	9	10	11	12	13	14	15
									Position in web							
Basis weight, g/m^2		50.1	50.4	51.6	52.2	52.9	52.4	53.6	--	53.9	53.8	53.6	53.6	54.4	54.7	54.1
Thickness, µm		86	88	87	88	89	90	90	--	91	91	91	91	91	91	91
Tensile strength, N/m	MD	2220	2490	2610	2660	2610	2690	2790	--	--	3240	3200	3230	3260	3330	3290
	CD	1580	--	--	--	--	--	--	--	--	--	--	--	--	--	1630
Stretch, %	MD	1.07	1.19	1.16	1.13	1.09	1.16	1.16	--	--	1.20	1.16	1.13	1.13	1.17	1.14
	CD	5.29	--	--	--	--	--	--	--	--	--	--	--	--	--	5.24
TEA, kg-m/m^2	MD	1.56	1.97	2.02	2.00	1.89	2.12	2.16	--	--	2.58	2.47	2.50	2.54	2.58	2.50
	CD	6.56	--	--	--	--	--	--	--	--	--	--	--	--	--	6.75
Et, kN/m	MD	323	353	363	380	375	379	395	--	--	442	447	449	459	459	450
	CD	154	--	--	--	--	--	--	--	--	--	--	--	--	--	155
Zero-span tensile strength, kg/cm	MD	7.01	--	--	7.20	--	--	--	8.08	--	--	--	8.09	--	--	8.61
	CD	5.59	--	--	5.67	--	--	--	5.30	--	--	--	5.15	--	--	5.24
In-plane tear, g-cm/cm	MD	--	135	--	--	131	--	--	119	--	--	120	--	--	118	--
	CD	--	100	--	--	108	--	--	114	--	--	110	--	--	111	--

TABLE XX

PHYSICAL PROPERTIES OF BOND PAPER AT VARIOUS RELATIVE HUMIDITIES

Relative Humidity, %

		12		50		(85)50 Position in web		76		85	
		1	15	1	15	1	15	1	15	1	15
Basis weight, g/m^2		73.8	73.3	74.4	73.2	76.3	75.1	77.3	77.4	78.4	78.5
Thickness, μm		100	99	101	101	106	107	107	108	109	109
Tensile strength, N/m	MD	4510	4500	3860	3850	3770	3580	2950	2970	2510	2360
	CD	3110	3200	2550	2490	2440	2570	2000	1940	1710	1720
Stretch, %	MD	1.12	1.15	1.44	1.47	1.56	1.43	1.62	1.62	1.72	1.50
	CD	1.91	1.92	2.78	2.62	2.84	2.34	3.88	3.74	3.99	4.16
TEA, $kg\text{-}m/m^2$	MD	3.05	3.17	3.59	3.65	3.81	3.34	3.22	3.23	2.93	2.41
	CD	4.27	4.29	5.39	4.95	5.25	6.53	5.80	5.46	5.03	5.19
E_t, kN/m	MD	610	601	534	533	511	506	418	425	406	401
	CD	414	416	370	366	338	342	285	283	230	228
Zero-span tensile strength, kg/cm	MD	9.28	9.07	8.97	9.33	9.76	9.38	8.65	8.84	8.84	8.70
	CD	8.49	8.26	8.29	8.34	7.60	8.14	8.01	7.58	7.94	7.60
In-plane tear, g-cm/cm	MD	60.6	61.8	75.6	74.0	79.8	77.0	77.8	78.0	74.2	73.8
	CD	55.6	55.2	67.0	68.4	69.8	72.6	72.0	70.4	69.2	65.6
Elmendorf tear, g	MD	49.8	40.0	50.4	51.8	58.2	59.4	64.2	66.8	67.0	60.6
	CD	36.8	39.8	50.0	53.2	55.4	55.8	54.0	58.4	57.6	55.6
Moisture content, %		2.9		5.9		6.4		8.6		10.3	

The test material, stored at 50% RH and 23°C, was exposed directly to the designated relative humidities, conditioned for at least 48 hours, and then tested. In one case, identified as (85)50, the test material was preconditioned at 85% RH and then conditioned and tested at 50% RH. The temperature in all cases was 23°C. The stretch, TEA, and E_t results have been corrected for instrumental strain error.

TABLE XXI

SUMMARY OF AVERAGE PHYSICAL PROPERTIES OF FOUR PAPERS AT 50% RH

		Offset	Bond	Kraft	Bag[a]
Basis weight, g/m^2		47.8	74.0	82.5	52.9
Thickness, μm		60	101	80.4	89.5
Tensile strength, N/m	MD	2930	3800	9780	--
(Instron)	CD	1550	2520	4085	--
Stretch, %	MD	1.51	1.42	2.31	1.15
	CD	3.83	2.70	4.41	5.25
TEA, $kg-m/m^2$	MD	2.93	3.49	14.3	--
	CD	4.59	5.17	12.3	--
Extensional stiffness,	MD	420	531	892	--
$\underline{Et}$, kN/m	CD	212	368	299	--
Zero-span tensile	MD	6.30	9.08	15.5	--
strength, kg/cm	CD	4.90	8.26	8.1	--
In-plane tear, g-cm/cm	MD	54.5	74.8	67.5	--
	CD	53.6	67.7	95.7	--
Elmendorf tear, g-cm/cm	MD	61.8	102.2	86.6	--
	CD	56.6	103.2	113.2	--
Ash content, % at 550° C		11.5	7.77	1.70	--
925° C		--	7.70	1.50	0.8
Average fiber length, mm					
Arithmetic		1.22	1.31	1.46	1.77
Length weighted		1.83	1.57	1.97	2.56

---

[a]Refer to Table XIX.